Contents lists available at SciOpen

Food Science and Human Wellness

journal homepage: https://www.sciopen.com/journal/2097-0765

Sugarcane leaves-derived polyphenols alleviate metabolic syndrome and modulate gut microbiota of *ob*/*ob* mice

Li Sun[a,b,1], Tao Wang[a,b,1], Baosong Chen[a,b], Cui Guo[a,b], Shanshan Qiao[a,b], Jinghan Lin[a,b], Huan Liao[a,b], Huanqin Dai[a,b], Bin Wang[c], Jingzu Sun[a,*], Hongwei Liu[a,b,*]

[a] *State Key Laboratory of Mycology, Institute of Microbiology, Chinese Academy of Sciences, Beijing 100101, China*
[b] *Savaid Medicine School, University of Chinese Academy of Sciences, Beijing 100101, China*
[c] *Guangxi Academy of Sciences, Nanning 530007, China*

ARTICLE INFO

Article history:
Received 5 July 2022
Received in revised form 22 August 2022
Accepted 21 September 2022
Available Online 25 September 2023

Keywords:
Sugarcane leaves-derived polyphenols
Metabolic syndrome
Bacteroides acidifaciens
Akkermansia muciniphila
Secondary bile acids metabolism

ABSTRACT

Sugarcane leaves-derived polyphenols (SLP) have been demonstrated to have diverse health-promoting benefits, but the mechanism of action has not been fully elucidated. This study aimed to investigate the anti-metabolic disease effects of SLP and the underlying mechanisms in mice. In the current study, we prepared the SLP mainly consisting of three flavonoid glycosides, three phenol derivatives, and two lignans including one new compound, and further demonstrated that SLP reduced body weight gain and fat accumulation, improved glucose and lipid metabolism disorders, ameliorated hepatic steatosis, and regulated short-chain fatty acids (SCFAs) production and secondary bile acids metabolism in *ob*/*ob* mice. Notably, SLP largely altered the gut microbiota composition, especially enriching the commensal bacteria *Akkermansia muciniphila* and *Bacteroides acidifaciens*. Oral gavage with the above two strains ameliorated metabolic syndrome (MetS), regulated secondary bile acid metabolism, and increased the production of SCFAs in high-fat diet (HFD)-induced obese mice. These results demonstrated that SLP could be used as a prebiotic to attenuate MetS via regulating gut microbiota composition and further activating the secondary bile acids-mediated gut-adipose axis.

1. Introduction

Metabolism syndrome (MetS) consists of a group of metabolic risk factors including abdominal obesity, hyperlipidemia, insulin resistance, hypertension, and hepatic steatosis. Epidemiological studies indicated that at least 25 percent of the world's adults suffered from MetS, which has become a major health-threatening[1-2]. The mechanisms that trigger MetS are complex and have been proven to be associated with chronic low-grade inflammation, chronic stress, dyslipidemia, endothelial dysfunction, hypertension, insulin resistance, and visceral obesity[3-4]. The present treatments for MetS including drugs (berberine, metformin, orlistat, etc.) and bariatric surgery are limited due to their poor efficacy and some undesirable side effects. Therefore, exploring and developing new, safe drugs or therapeutic strategies to combat MetS is robustly needed.

Growing evidences have shown that gut microbiota plays a crucial role in the development and progression of MetS. The intestinal microbiota consists of trillions of microbes that profoundly influence nutrient acquisition and energy metabolism. Compared to non-obese individuals, the obese subjects have an increased Firmicutes to Bacteroidetes ratio (F/B ratio)[5]. Another study reported that gut microbiota dysbiosis impaired intestinal barrier, which led to the release of lipopolysaccharide (LPS) into the circulation system, resulting in systemic inflammation and insulin resistance[6]. Many gut microbiota-derived metabolites, especially short-chain fatty

[1] These authors contributed equally.
[*] Corresponding authors at: State Key Laboratory of Mycology, Institute of Microbiology, Chinese Academy of Sciences, Beijing 100101, China.
E-mail address: liuhw@im.ac.cn (H.W. Liu); sunjz@im.ac.cn (J.Z. Sun)
Peer review under responsibility of Tsinghua University Press.

Publishing services by Tsinghua University Press

http://doi.org/10.26599/FSHW.2022.9250048

acids (SCFAs), bile acids, and branched-chain amino acids (BCAAs) have been implicated in the development of metabolic disorders. SCFA-producing bacteria, such as *Akkermansia muciniphila* and *Faecalibacterium prausnitzii*, and *Faeciroseburia intestinalis* were confirmed to reduce MetS by increasing energy expenditure, improving glucose tolerance, and maintaining host homeostasis[7-9]. The gut commensal *Parabacteroides distasonis* was reported to reduce obesity, hyperglycemia, and nonalcoholic fatty liver disease via the production of succinate acid and secondary bile acids[10]. On the other hand, *Prevotella copri* was found to increase circulating levels of BCAAs, leading to insulin resistance and glucose intolerance[11]. Thus, regulating the gut microbiota or the gut microbiota-derived metabolites is proposed as a novel therapy to prevent or treat MetS.

Dietary intervention has been an effective strategy to control metabolic syndrome by regulating the composition of gut microbes. Epidemiological investigations have presented a negative correlation between dietary polyphenols with low bioavailability and the development of MetS[12]. For instance, supplementation of theabrownin could attenuate hypercholesterolemia by inhibiting the farnesoid X receptor (FXR)-fibroblast growth factor 15 (FGF15) signaling pathway and modulating gut microbiota associated with bile-salt hydrolase (BSH) activity[13]. Resveratrol can prevent obesity in HFD-fed mice by regulating the composition of gut bacterial community and redox status of the intestinal environment[14]. Clinical trials have also shown that dietary polyphenols can help control hyperglycemia and dyslipidemia in type 2 diabetes[15].

Sugarcane leaves are an undervalued by-product in the sugar industry and generally used as animal feeds[16]. In this study, we attempted to study the effects of sugarcane leaves-derived polyphenols (SLP) on MetS in *ob*/*ob* mice. We also aimed to understand the relationship between the gut microbiota and the salutary effects of SLP. SLP was prepared and chemically characterized by three flavonoid glycosides, three phenol derivatives, and two lignans including one new compound. Our results showed that SLP significantly decreased body weight, fat accumulation, and hyperlipidemia, ameliorated hyperglycemia and metabolic endotoxemia, and maintained intestinal barrier integrity. We further found that the anti-MetS effects of SLP were relevant to the adjustment of gut microbiota and secondary bile acids metabolism. Gavage with the strains of *Bacteroides acidifaciens* and *A. muciniphila* enriched by SLP treatment effectively alleviated MetS. These results confirmed the therapeutic efficacy of SLP in MetS and revealed an important relationship between polyphenols, gut microbiota, and MetS.

2. Materials and methods

2.1 Materials and instruments

The sugarcane leaves samples were collected in the Guangxi Zhuang Autonomous Region of China. Samples were transported under refrigeration, and dried by air. Tea polyphenols were purchased from Solarbio (Beijing, China). The 1D and 2D NMR spectras were recorded on a Bruker Avance-500 spectrometer. HRESIMS data were measured by using an Agilent Accurate-Mass-Q-TOF LC/MS 6520 instrument. CD spectra were acquired using an Applied Photophysics Chirascan spectropolarimeter. PCR amplification was performed in a Bio-Rad/My cycler thermal cycler. D-101 macroporous adsorption resins (Tianjin Bohong Resin Technology CO., Ltd.), polyamide (Polyram), octadecylsilyl (ODS, 50 μm, YMC CO., LTD), and Sephadex LH-20 (Amersham Biosciences) used for column chromatography were purchased commercially.

2.2 Preparation of the SLP from sugarcane leaves

The dried sugarcane leaves were cut into small pieces and 4.4 kg pieces of dried sugarcane leaves were soaked and extracted three times at 100 °C with 50 L of water for 3 h. The combined solvents were condensed to about 2 L under vacuum and subjected to a D-101 macroporous adsorption resin column (50 mm × 500 mm) using gradient elution with 0, 30%, 50%, and 70% ethanol in distilled water (each 10 L). Each eluent was combined to obtain four fractions (Fr. 1 to Fr. 4). By thin layer chromatography (TLC) and high-performance liquid chromatography (HPLC) analysis, SLP was found in the Fr. 3. Then, Fr. 3 (16.5 g) were separated by ODS column chromatography (CC) eluted with MeOH in water (from 10% to 50%, *V*/*V*). The collected elution was combined by TLC and HPLC analysis into 4 fractions (Fr. 3-1 to Fr. 3-4). SLP was found to be rich in Fr. 3-1 according to color reaction with $FeCl_3$ on TLC and ultraviolet spectrum recorded by HPLC analysis. 0.5 g of SLP was used to further chemical investigation. 6.1 g of SLP was used for animal experiments.

The chromatographic separation of SLP was injected at 10 μL on Waters Alliance e2695 separation module equipped with Kromasil 100-5-C4 (250 mm × 4.6 mm, 5 μm). The mobile phase consisted methanol (phase A) and water with 1% trifluoroacetic (phase B); linear gradient: 0–12 min, 15%–20% A in B; 12–90 min, 20%–35% A in B; 90–95 min, 100% A. The flow rate was 1 mL/min with column temperature at 35 °C.

2.3 Separation and identification of polyphenols in SLP

Fr. 3-1 (0.5 g) was eluted with MeOH in water (from 60% to 100%, *V*/*V*) on Sephadex LH-20 to give 20 fractions (Fr. 3-1-1–Fr. 3-1-20). Compound **2** (24.9 mg) was directly obtained from Fr. 3-1-15 eluted with 90% MeOH in water. Used a polyamide column eluted with MeOH in water (from 0 to 100%, *V*/*V*) to purify Fr. 3-1-5 (188.4 mg, 70% MeOH elution) in 6 subfractions (Fr. 3-1-5-1–Fr. 3-1-5-6). Compounds **5** (1.7 mg, t_R = 58.8 min) and **6** (2.4 mg, t_R = 63.1 min) were further purified by RP-HPLC (C_8, 5 μm, 4.6 mm × 250 mm, Agilent) using 35% MeOH in water from Fr. 3-1-5-2 (16.7 mg, 20% MeOH elution). Compounds **7** (2.9 mg, t_R = 77.4 min) and **8** (1.9 mg, t_R = 86.6 min) were obtained by RP-HPLC (C_{18}, 5 μm, 4.6 mm × 250 mm, Agilent) using 42% MeOH in water from Fr. 3-1-5-5 (19.1 mg, 80% MeOH elution). Fr. 3-1-10 (16.0 mg, 80% MeOH elution) was separated by RP-HPLC (C_{18}, 5 μm, 4.6 mm × 250 mm, Agilent) using 32% methanol in water to give compound **1** (2.2 mg, t_R = 20.2 min). Fr. 3-1-13 (79.2 mg, 90% MeOH elution) was further separated by preparative TLC with chloroform/methanol (10: 1, *V*/*V*) to give 5 subfractions (Fr. 3-1-13-1–Fr. 3-1-13-5). Fr. 3-1-13-1 (17.6 mg) and Fr. 3-1-13-4 (12.1 mg) were purified by RP-HPLC (C_{18}, 5 μm, 4.6 mm × 250 mm, Agilent) using 40% methanol in water to give compounds **3** (3.2 mg, t_R = 21.6 min) and **4** (1.7 mg, t_R = 24.3 min), respectively.

4-Hydroxybenzaldehyde (**1**), $C_7H_6O_2$, yellow solid. ^{1}H NMR (500 MHz, DMSO-d_6): δ 10.60 (1H, s), 9.79 (1H, s), 7.75 (2H, d, J = 8.5 Hz), 6.92 (2H, d, J = 8.0 Hz). Positive HRESIMS m/z 123.045 8 $[M + H]^+$ (calcd for $C_7H_7O_2$, 123.044 6). Compound **1** was identified as 4-hydroxybenzaldehyde by comparing NMR data with the literature[17].

p-Coumaric acid (**2**), $C_9H_8O_3$, white amorphous powder. ^{1}H NMR (500 MHz, CD_3OD): δ 7.60 (1H, d, J = 16.0 Hz), 7.44 (2H, d, J = 8.0 Hz), 6.80 (2H, d, J = 8.0 Hz), 6.27 (1H, d, J = 16.0 Hz). ^{13}C NMR (125 MHz, CD_3OD): δ 170.7, 160.8, 146.3, 130.7, 130.7, 126.9, 116.5, 116.5, 115.2. Positive HRESIMS m/z 165.0553 $[M + H]^+$ (calcd for $C_9H_9O_3$, 165.055 2). Compound **2** was identified by comparing NMR data with literature[18-19].

(*E*)-3-(4-Hydroxy-3-methoxyphenyl) acrylic acid (**3**), $C_{10}H_{10}O_4$, white amorphous powder. ^{1}H NMR (500 MHz, DMSO-d_6): δ 12.11 (1H, s), 9.53 (1H, s), 7.47 (1H, d, J = 15.9 Hz), 7.27 (1H, d, J = 2.0 Hz), 7.07 (1H, dd, J = 8.1, 2.0 Hz), 6.78 (1H, d, J = 8.1 Hz), 6.35 (1H, d, J = 15.9 Hz), 3.81 (3H, s); ^{13}C NMR (125 MHz, DMSO-d_6): δ 167.9, 148.9, 147.7, 144.3, 125.6, 122.7, 115.6, 115.3, 111.0, 55.5. Positive HRESIMS m/z 195.065 9 $[M + H]^+$ (calcd for $C_{10}H_{11}O_4$, 195.065 7). Compound **3** was identified by comparing NMR data with the literature[20].

Sugarcanoic acid (**4**), $C_{20}H_{20}O_7$, yellow amorphous powder. ^{1}H NMR (500 MHz, DMSO-d_6): δ 9.35 (1H, s, 6-OH), 8.70 (1H, s, 4′-OH), 7.46 (1H, s, H-1), 7.03 (1H, s, H-8), 6.61 (1H, d, J = 2.0 Hz, H-2′), 6.60 (1H, s, H-5), 6.54 (1H, d, J = 8.0 Hz, H-5′), 6.17 (1H, dd, J = 2.0, 8.0 Hz, H-6′), 4.22 (1H, s, H-4), 3.78 (3H, s, H-3′-OCH_3), 3.66 (3H, s, H-7-OCH_3), 3.42 (1H, dd, J = 4.0, 10.3 Hz, H-10), 2.97 (1H, dd, J = 4.0, 10.3 Hz, H-3), 2.89 (1H, t, J = 10.3 Hz, H-10); ^{13}C NMR (125 MHz, DMSO-*d*6): δ 167.1 (C-9), 148.9 (C-6), 147.7 (C-3′), 146.9 (C-7), 145.2 (C-4′), 137.1 (C-1), 136.6 (C-1′), 131.3 (C-4a), 125.5 (C-2), 123.5 (C-8a), 119.9 (C-6′), 117.7 (C-5), 115.6 (C-5′), 113.2 (C-8), 112.1 (C-2′), 61.3 (C-10), 56.2 (C-3′-OCH_3), 56.1 (C-7-OCH_3), 45.0 (C-3), 42.5 (C-4). Positive HRESIMS m/z 373.128 5 $[M + H]^+$ (calcd for $C_{20}H_{21}O_7$, 373.128 7).

Isoviolanthin (**5**), $C_{27}H_{30}O_{14}$, yellow amorphous powder. ^{1}H NMR (500 MHz, DMSO-d_6): δ 8.00 (2H, d, J = 8.8 Hz), 6.89 (2H, d, J = 8.8 Hz), 6.81 (1H, s), 5.28 (1H, s), 4.85 (1H, d, J = 9.8 Hz), 1.17 (3H, d, J = 6.3 Hz), 3.00-4.00 (10 H, m, sugar protons); ^{13}C NMR (125 MHz, DMSOJ-d_6): δ 182.8, 164.6, 161.7, 161.4, 158.0, 155.5, 129.5, 129.5, 122.0, 116.3, 116.3, 108.8, 105.6, 104.2, 103.1, 82.3, 79.4, 76.5, 75.1, 74.5, 73.7, 71.6, 71.3, 71.0, 69.9, 61.7, 17.5. Positive HRESIMS m/z 579.170 6 $[M + H]^+$ (calcd for $C_{27}H_{31}O_{14}$, 579.171 4). Compound **7** was identified by comparing NMR and MS data with the literature[21].

(+)-Syringaresinol-*O*-*D*-glucopyranoside (**6**), $C_{28}H_{36}O_{13}$, white amorphous powder. ^{1}H NMR (500 MHzi, C_5D_5N): δ 7.00 (2H, s), 6.97 (2H, s), 5.83 (1H, dd, J = 7.0, 4.0 Hz), 5.00 (2H, t, J = 5.0 Hz), 4.31-4.43 (7H, m), 4.08 (2H, m), 3.96 (1H, m), 3.85 (6H, s), 3.82 (6H, s), 3.20-3.30 (2H, m); ^{13}C NMR (125 MHz, C_5D_5N): δ 154.1, 154.1, 149.4, 149.4, 138.5, 137.4, 132.2, 132.2, 105.2, 105.0, 104.9, 104.9, 104.9, 86.7, 86.4, 78.8, 78.5, 76.2, 72.3, 72.2, 71.7, 62.7, 56.8, 56.8, 56.6, 56.6, 55.1, 55.0. Positive HRESIMS m/z 603.200 1 $[M + Na]^+$ (calcd for $C_{28}H_{36}O_{13}Na$, 603.205 4). Compound **6** was identified by comparing NMR and MS data with the literature[22].

Tricin-7-*O*-*β*-*D*-glucopyranoside (**7**), $C_{23}H_{24}O_{12}$, yellow amorphous powder. ^{1}H NMR (500 MHz, DMSO-d_6): δ 12.95 (1H, s), 9.40 (1H, s), 7.36 (2H, s), 7.08 (1H, s), 6.93 (1H, d), 6.46 (1H, d, J = 2.1 Hz), 5.05 (1H, d, J = 7.4 Hz), 3.88 (6H, s); ^{13}C NMR (125 MHz, DMSO-d_6): δ182.1, 164.1, 163.2, 161.1, 156.9, 148.2, 148.2, 140.1, 120.2, 105.3, 104.5, 104.5, 103.8, 100.2, 99.4, 95.3, 77.4, 76.5, 73.2, 69.6, 60.7, 56.4, 56.4. Positive HRESIMS m/z 493.136 5 $[M + H]^+$ (calcd for $C_{23}H_{25}O_{12}$, 493.134 6). Compound **7** was identified by comparing NMR data with the literature[23].

Tricin-7-*O*-neohesperidoside (**8**), $C_{29}H_{34}O_{16}$, yellow amorphous powder. ^{1}H NMR (500 MHz, DMSO-d_6): δ12.90 (1H, s), 9.40 (1H, s), 7.33 (2H, s), 7.01 (1H, s), 6.89 (1H, d, J = 2.2 Hz), 6.38 (1H, d, J = 2.2 Hz), 5.21 (1H, d, J = 7.4 Hz), 5.11 (1H, s), 3.88 (6H, s), 1.18 (3H, d, J =6.2 Hz); ^{13}C NMR (125 MHz, DMSO-d_6): δ 182.1, 164.1, 162.7, 161.1, 157.0, 148.2, 148.2, 140.1, 120.2, 105.5, 104.5, 104.5, 104.0, 100.5, 99.5, 98.2, 94.9, 77.3, 77.2, 76.4, 71.9, 70.5, 70.4, 69.8, 68.4, 60.5, 56.4, 56.4, 18.0. Positive HRESIMS m/z 639.191 4 $[M + H]^+$ (calcd for $C_{29}H_{35}O_{16}$, 639.192 5). Compound **8** was identified by comparing NMR and MS data with the literature[24].

2.4 Animal experiments and bacteria strains

Six-week-old male C57BL/6J mice and *ob*/*ob* (leptin deficiency) mice were purchased from the Experimental Animal Center, Chinese Academy of Medical Sciences. Mice were fed with a chow diet (NCD, 13.5% calories from fat) or a high-fat diet (HFD, 60 kcal% fat as indicated, Catalog D12492, Research Diet, New Brunswick, NJ, USA). All the animal studies were approbated by the Institute of Microbiology, Chinese Academy of Sciences (IMCAS). All mice were housed in a pathogen-free facility with a 12 h light/dark cycle.

For the efficacy assay of SLP treatment on *ob*/*ob* mice, 8-week-old males were sorted into 5 groups (n = 10 each) after 2 weeks of acclimatization: the group of C57BL/6J mice was treated with distilled water (Lean), the group of *ob*/*ob* mice was treated with distilled water (MOD), the group of *ob*/*ob* mice was treated with 50 mg/kg·day SLP (SLPL), the group of *ob*/*ob* mice was treated with 100 mg/kg·day SLP (SLPH) and the group of *ob*/*ob* mice was treated with 50 mg/kg·day tea polyphenols (TP). Treatments lasted for 6 weeks.

For evaluation of *B. acidifaciens* and *A. muciniphila* on high-fat diet-induced obese (DIO) mice, the experiment started after feeding with a high-fat diet for 10 weeks. *A. muciniphila* (provided by Dr. Biao Ren from West China Stomatological Hospital) and *B. acidifaciens* (JCM 10556, Japan Collection of Microorganisms) were propagated overnight at 37 °C in anaerobic brain-heart infusion (BHI) broth and modified GAM broth, respectively. The *A. muciniphila* and *B. acidifaciens* were diluted in oxygen-free PBS with a final concentration of 1×10^8 CFU/mL. Briefly, 5 experimental groups were set: 10 C57BL/6J mice treated with PBS (CON), each 10 DIO mice were treated with PBS, *B. acidifaciens* and *A. muciniphila*, and a combination of *A. muciniphila* and *B. acidifaciens*, respectively. Each mouse was orally given 200 μL of the prepared bacterial solution. Treatments lasted for 7 weeks.

Animals in each group were subjected to the oral glucose tolerance test (OGTT) and an insulin tolerance test (ITT) test before cervical dislocation sacrificed. At the end of the experiments, mice were sacrificed for cervical dislocation. Blood and tissue samples were collected, weighed, and frozen immediately in liquid nitrogen and then stored at −80 °C for subsequent analysis. For fecal sample collection, the mice were placed into an empty cage with no bedding

for 4 h. The fresh fecal samples were put into test tubes, then stored at −80 °C for analysis.

2.5 Histological analysis

After euthanasia and bleeding of mice, liver, subcutaneous adipose tissues, and small intestine tissues were dissected, and then put into 2 mL 4% paraformaldehyde solution for 48 h. Paraffin-embedded tissues were frozen and sliced into 5–7 μm sections. Oil red staining and hematoxylin-eosin staining were respectively conducted on frozen sections to assess hepatic and subcutaneous white adipose tissues (WAT). Alcian blue periodic acid Schiff (AB-PAS) was used to stain the small intestine tissues following the procedure described previously[25].

2.6 Biochemical analysis

Plasma was obtained by centrifugation of supernatant in a heparin tube at 3 000 × *g* for 15 min. For the liver histological analysis, the liver homogenate was prepared with 10% (*m*/*V*) and centrifuged at 3 000 × *g* for 15 min at 4 °C to obtain the supernatant. Plasma and hepatic high-density lipoprotein cholesterol (HDL-C), total cholesterol (TC), triglycerides (TG), and low-density lipoprotein cholesterol (LDL-C) were determined using commercial kits., Plasma aspartate aminotransferase (AST), alanine aminotransferase (ALT), tumor necrosis factor (TNF-α), interleukin 10 (IL-10), LPS, insulin, glycated hemoglobin, interleukin 6 (IL-6), and interleukin-1β (IL-1β) levels, as well as hepatic total antioxidant capacity (T-AOC), superoxide dismutase (SOD), glutathione (GSH), and malondialdehyde (MDA) were determined as described previously[26]. The insulin sensitivity index (ISI) was calculated from the values of fasting blood glucose (FBG, in mg/dL), and fasting blood insulin (FBI, in mU/L) was used to calculate the insulin sensitivity index.

$$\mathrm{ISI} = \frac{1}{1\,000 \times \mathrm{FBI} \times \mathrm{FBG}}$$

2.7 Real-time qPCR analysis

The qPCR analysis was performed as described previously[26]. Total RNA of the adipose tissues and ileum tissue was extracted using the TRIzol (Invitrogen, Carlsbad, CA, USA) and cDNA was obtained using the reverse transcription cDNA synthesis kit (Tiangen, Beijing, China). All primer sequences were listed in Table S1. Relative mRNA expression was normalized by glyceraldehyde-3-phosphate dehydrogenase (*Gapdh*). The $2^{-\Delta\Delta Ct}$ method was used to determine the relative quantification expression of targeted genes.

2.8 Analysis of gut microbiota by 16S rRNA sequencing

The fecal DNA was extracted using a QIAamp Fast DNA stool Mini Kit (Qiagen, Cat# 51604). The primer pairs 341F (CCTAYGGGRBGCASCAG) and 806R (GGACTACNNGGGTATCTAAT) were used to amplify the variable region 3-4 (V3-V4) of the 16S rRNA gene. The pair-end library was set up and sequenced based on the Illumina NovaSeq sequencing platform[27-29]. Raw 16S rDNA data had been deposited on gcMeta[30] at https://nmdc.cn/ with project ID NMDC10018134.

2.9 SCFA analysis

Fifty microgram of freeze-drying fecal sample was resuspended in 1 mL methanol, mixed thoroughly, and centrifuged at 4 000 × *g* for 15 min. The supernatant was subjected to GC-MS analysis[10] to measure the levels of SCFAs.

2.10 Fecal bile acid analysis

One hundred microgram of lyophilized feces dissolved in 1 mL methanol, mixed thoroughly, and centrifuged at 4 000 × *g* for 15 min. The supernatants obtained were analyzed on a Waters Alliance e2695 separation module with a 2424 ELSD Detector equipped with a C_{18} column (5 μm, 4.6 mm × 250 mm, Agilent) according to a previous report[26].

2.11 Statistical analysis

All data are expressed as the mean ± SEM. Results were assessed by two-tailed unpaired Student's *t*-test and two-way ANOVA, and the *P* values < 0.05 were considered significant. SPSS 22.0 software was used for Pearson correlation analysis to determine the relationship between variables. GraphPad Prism version 7.0 (GraphPad Software Inc., La Jolla, CA) was employed for drawing.

3. Results

3.1 Preparation of SLP and identification of polyphenols compounds in SLP

In this study, the water crude extract of 4.4 kg dry sugarcane leaves was chromatographed on a D101-macroporous resin column and further separated by ODS column chromatography to give sugarcane leaves-derived polyphenols (SLP, 6.6 g). Then, 0.5 g SLP was separated by LH-20 and polyamide column chromatography and further RP-HPLC purification, and 8 polyphenol compounds were obtained from SLP (Fig. 1A). Compounds **1**–**3**, **5**–**8** were established as 4-hydroxybenzaldehyde (**1**); *p*-coumaric acid (**2**); (*E*)-3-(4-hydroxy-3-methoxyphenyl) acrylic acid (**3**); isoviolanthin (**5**); (+)-syringaresinol-*O*-*D*-glucopyranoside (**6**); tricin-7-*O*-*β*-*D*-glucopyranoside (**7**); tricin-7-*O*-neohesperidoside (**8**) in comparison of NMR and MS data with the literature data. The new lignan compound, sugarcanoic acid (**4**), was assigned by the analysis of NMR, MS, specific rotation, and ECD spectrum. Compounds **1**–**8** which accounted for the largest proportion of SLP were identified in the HPLC fingerprint chromatogram and accounted for 11.96%, 34.63%, 0.83%, 1.93%, 3.88%, 2.03%, 0.89%, and 3.92% in the total peak area (Fig. 1B).

The molecular formula of sugarcanoic acid (**4**) (yellow amorphous powder) was determined to be $C_{20}H_{20}O_7$ according to the HRESIMS data at *m*/*z* 373.128 5 $[M + H]^+$ (calcd for $C_{20}H_{21}O_7$, 373.128 7). The ^{1}H NMR spectrum (Fig. S1) revealed the presence of six aromatic or olefinic protons including three singlet signals at *δ* 7.46, 7.03 and 6.60 and one group ABX signals at *δ* 6.61 (d, *J* = 2.0 Hz), 6.54 (d, *J* = 8.0 Hz), and 6.17 (dd, *J* = 2.0, 8.0 Hz), one singlet proton at *δ* 4.22, two oxygenated methyls at *δ* 3.66 and 3.78, and 3 mutually coupled protons at *δ* 2.89 (t, *J* = 10.3 Hz), 2.97 (dd, *J* = 4.0, 10.3 Hz) and 3.42 (dd, *J* = 4.0, 10.3 Hz). In the ^{13}C NMR spectrum (Fig. S2),

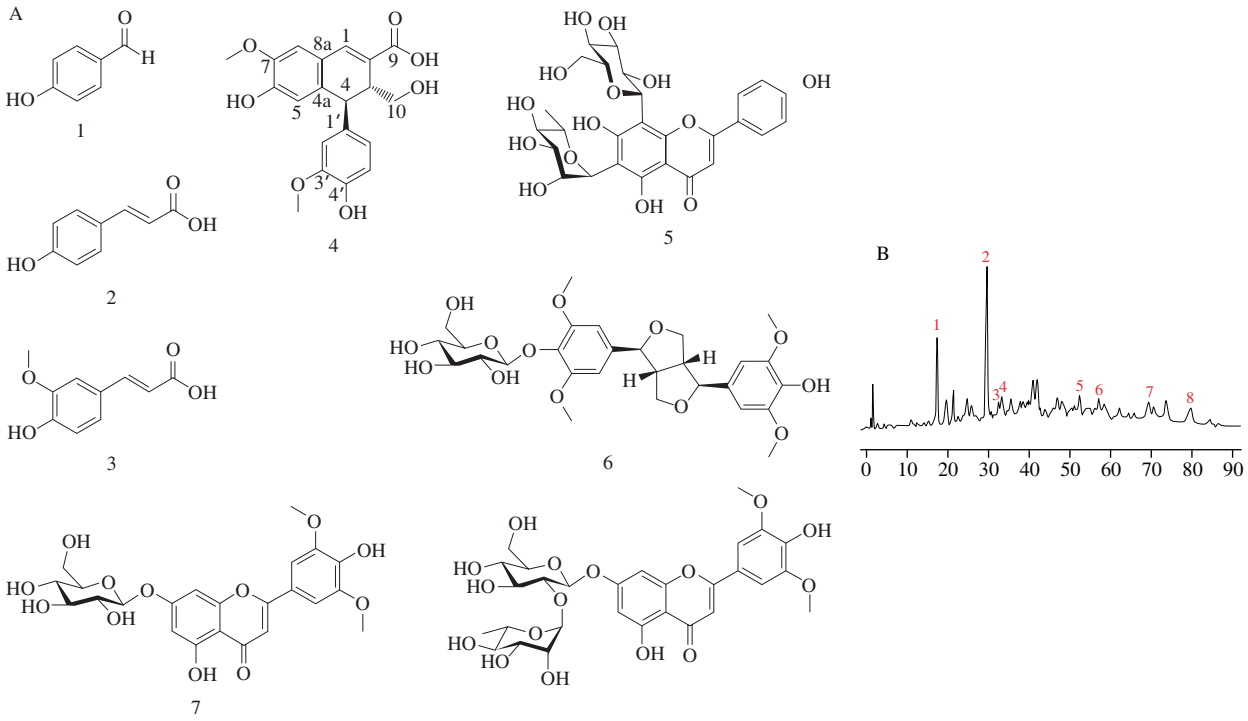

Fig. 1 HPLC chromatogram at 220 nm and the structure of sugarcane leaves-derived polyphenols (SLP). (A) The structure of major polyphenol compounds obtained in SLP. 4-Hydroxybenzaldehyde (**1**); *p*-coumaric acid (**2**); (*E*)-3-(4-hydroxy-3-methoxyphenyl) acrylic acid (**3**); sugarcanoic acid (**4**); isoviolanthin (**5**); (+)-syringaresinol-*O*-*D*-glucopyranoside (**6**); tricin-7-*O*-*β*-*D*-glucopyranoside (**7**); tricin-7-*O*-neohesperidoside (**8**); (B) HPLC fingerprint chromatogram of SLP.

20 carbon signals were observed and attributed to a carboxylic group (δ 167.1), 14 aromatic or olefinic carbons (δ 110–150), and five sp^3 carbons. In the HMBC spectrum (Fig. S3), the HMBC correlations of a 7-OCH_3 proton with C-7, and H-8 and H-5 with C-7, C-6, C-4[a], and C-8a, one 6, 7, 4a, 8a-tetrasubstitution benzene was constructed. The ABX protons combining the HMBC correlations of H-2′ with C-1′, C-6′, C-3′, and C-4′, H-6′ with C-1′, C-5′, C-4′, and C-2′, H-5′ with C-1′, C-6′, C-3′, and C-4′, and 3′-OCH_3 proton with C-3′, revealed the existence of 1′, 3′, 4′-trisubstitution benzene. ^{1}H-^{1}H COSY (Fig. S4) correlations of H-3 with H-4 and H_2-10 and HMBC correlations of H-4 with C-4a, C-8a, C-1′, C-2, C-3 and C-10, H-1 with C-4a, C-8a, C-8, C-2, C-3, and C-9, and H-3 with C-4a, C-1, C-2, C-9, C-1′, C-4, and C-10, spliced the two benzene moieties with other carbons. Taking the chemical shift of C-6 (δ 148.9) and C-5′ (δ 115.6), and the molecular formula into consideration, the planar structure was confirmed as a ferulate-coniferyl alcohol coupling compound whose arabinoside has been reported and analyzed by mass[31]. The relative configurations at C-4 and C-3 were assigned based on the coupling constant between H-4 and H-3. The near-to-zero coupling constant indicated the dihedral angle between H-4 and H-3 was about 90°. The optical rotation values near zero and the lack of significant Cotton effects in electronic circular dichroism (ECD) spectra supported sugarcanoic acid (**4**) to be racemic.

3.2 SLP reduced body weight gain, hyperlipidemia, and hepatic lipid accumulation in ob/ob mice

Early studies have shown that some polyphenol-rich diets could inhibit body weight gain, alleviate metabolic syndrome, and reduce the risk of diabetes[32-33]. To assess whether SLP displays similar effects on metabolic syndrome, the *ob/ob* mice were gavaged with SLP at a dose of 50 mg/kg or 100 mg/kg. Tea polyphenols (TP, 50 mg/kg) showing biological activities in alleviating diabetes, obesity, and the obesity-related diseases[34-35] were used to positive control. Both doses of SLP and TP significantly inhibited body weight gain ($P < 0.001$) (Figs. 2A, B) and these results were independent of changes in energy intake (Fig. 2C). Besides, oral administration of SLP attenuated excessive adipose deposition in subcutaneous fat, epididymal fat, and mesenteric fat, consistent with the reduction in body weight (Fig. 2D). The cell diameter of adipocytes in subcutaneous adipose tissues of SLP-treated mice was significantly smaller than that of *ob/ob* mice (Fig. 2G). Moreover, SLP at 100 mg/kg also ameliorated hyperlipidemia by reducing plasma TC ($P = 0.003\ 91$) and LDL-C ($P = 0.000\ 08$) (Fig. 2E). However, the level of TG was not affected by SLP treatment (Fig. 2F).

Nonalcoholic fatty liver disease (NAFLD) was generally regarded as a risk factor for MetS. We further determined the effect of SLP on hepatic lipid metabolism and liver injury. The levels of hepatic TC, TG, and LDL-C were decreased by 7.3% ($P = 0.02$), 7.9% ($P = 0.02$), and 17.9% ($P = 0.03$) in SLP-treated (100 mg/kg) group compared to those of the vehicle-treated group (Figs. 2H-I). Oil red O staining also revealed that SLP improved hepatic steatosis (Fig. 2L). In addition, SLP at 100 mg/kg reduced liver injury, in consideration of the reduction of 29.7% and 24.8% with ALT ($P = 0.017\ 9$) and AST ($P = 0.027\ 6$) (Figs. 2J-K). Meanwhile, SLP at 100 mg/kg supplementation significantly reduced the levels of MDA ($P = 0.041\ 3$) and increased the levels of T-AOC ($P = 0.021\ 5$), SOD ($P = 0.018\ 3$), and GSH ($P = 0.003\ 9$) in the liver, indicating that SLP can improve the redox homeostasis in *ob/ob* mice (Fig. S5). As mentioned above, these results indicated that SLP significantly reduced obesity, hyperlipidemia, and hepatic steatosis in mice.

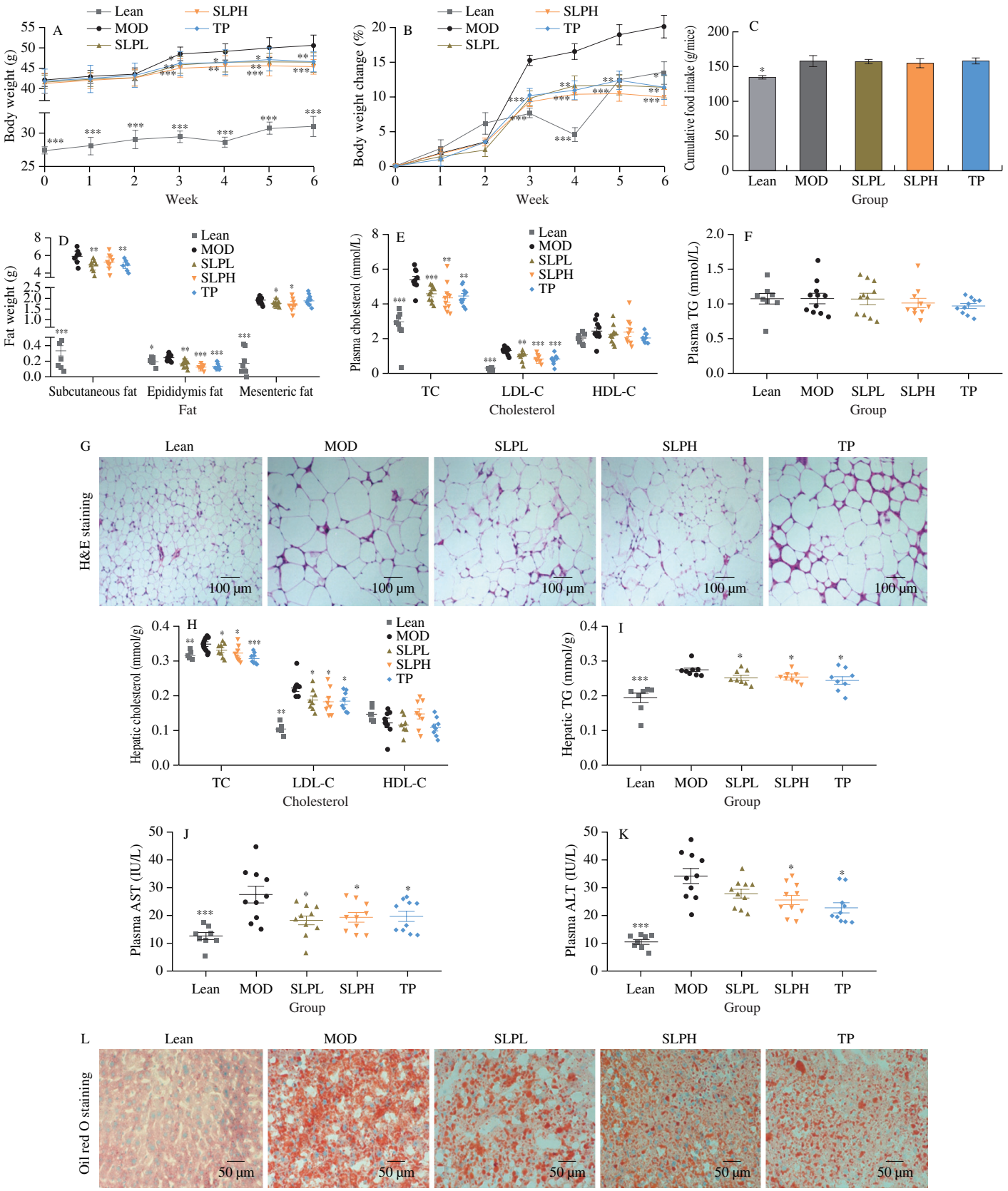

Fig. 2 SLP reduced body weight and fat accumulation and ameliorated hyperlipidemia and hepatic steatosis in *ob/ob* mice. *Ob/ob* mice were treated with distilled water, TP (50 mg/kg), or SLP (50 mg/kg or 100 mg/kg) for 6 weeks by daily oral gavage. (A) changes in body weight during 6 weeks; (B) body weight change; (C) cumulative food intake; (D) fat weight (subcutaneous fat; epididymis fat; mesenteric fat); (E) plasma TC, LDL-C, and HDL-C; (F) plasma TG; (G) representative H&E staining images of subcutaneous fat ($n = 5$; scale bars, 100 μm). (H) hepatic TC, LDL-C, and HDL-C; (I) hepatic TG; (J) plasma AST; (K) plasma ALT; (L) representative oil red O staining images of the liver ($n = 5$; scale bars, 50 μm). Statistical analysis was analyzed using unpaired Student's *t*-test for (C-F) and (H-K), and two-way ANOVA followed by the Bonferroni post hoc test for (A-B), $n = 10$. $^{*}P < 0.05$; $^{**}P < 0.01$; $^{***}P < 0.001$.

3.3 SLP improved hyperglycemia, inflammation, metabolic endotoxemia and maintained intestinal integrity in *ob/ob* mice

Growing evidence has shown that the leptin-deficient (*ob/ob*) mice exhibited an impaired glucose metabolism[36]. In this study, we found that SLPH supplementation significantly decreased the fasting diet blood glucose, plasma insulin, and glycosylated hemoglobin A1c (HbA1c) ($P < 0.05$) (Figs. 3A-C). Besides, SLP (100 mg/kg) treatment increased 2.2 times of insulin sensitivity, and improved glucose intolerance ($P = 0.020\ 0$) and insulin resistance ($P < 0.001$) (Figs. 3D-H).

Chronic low-grade inflammation is one of the major pathological factors of MetS. To assess the anti-inflammation effect of SLP, we measured the concentrations of cytokines including IL-6, IL-1β, IL-10, and TNF-α. SLP at 100 mg/kg treatment significantly decreased the levels of pro-inflammation cytokines (IL-6 and TNF-α) ($P < 0.05$) and increased the level of anti-inflammation cytokines (IL-10) ($P = 0.000\ 9$), but did not change the level of IL-1β (Figs. 3I-L).

Some studies have shown that the endotoxin LPS causes metabolic inflammation and insulin resistance when entering the circulation, and induces the occurrence and development of MetS[37]. We observed that the plasma LPS level was significantly decreased by 20.5% upon SLP (100 mg/kg) treatment ($P = 0.000\ 9$). Meanwhile, we also found that SLP at 100 mg/kg significantly up-regulated the expression of tight junction proteins (ZO-1, ZO-2, and Muc5) ($P < 0.05$) (Figs. 3M-N), revealing that SLP greatly enhanced intestinal barrier integrity. Additionally, Alcian Blue periodic acid Schiff (AB-PAS) staining confirmed that SLP could reverse the reduction of goblet cells in *ob/ob* mice ($P < 0.05$) as well as TP (Figs. 3O-P). Based on these results, we supposed that the improvement of gut barrier integrity by SLP contributes to the reduction of metabolic endotoxemia, thus decreasing hyperglycemia.

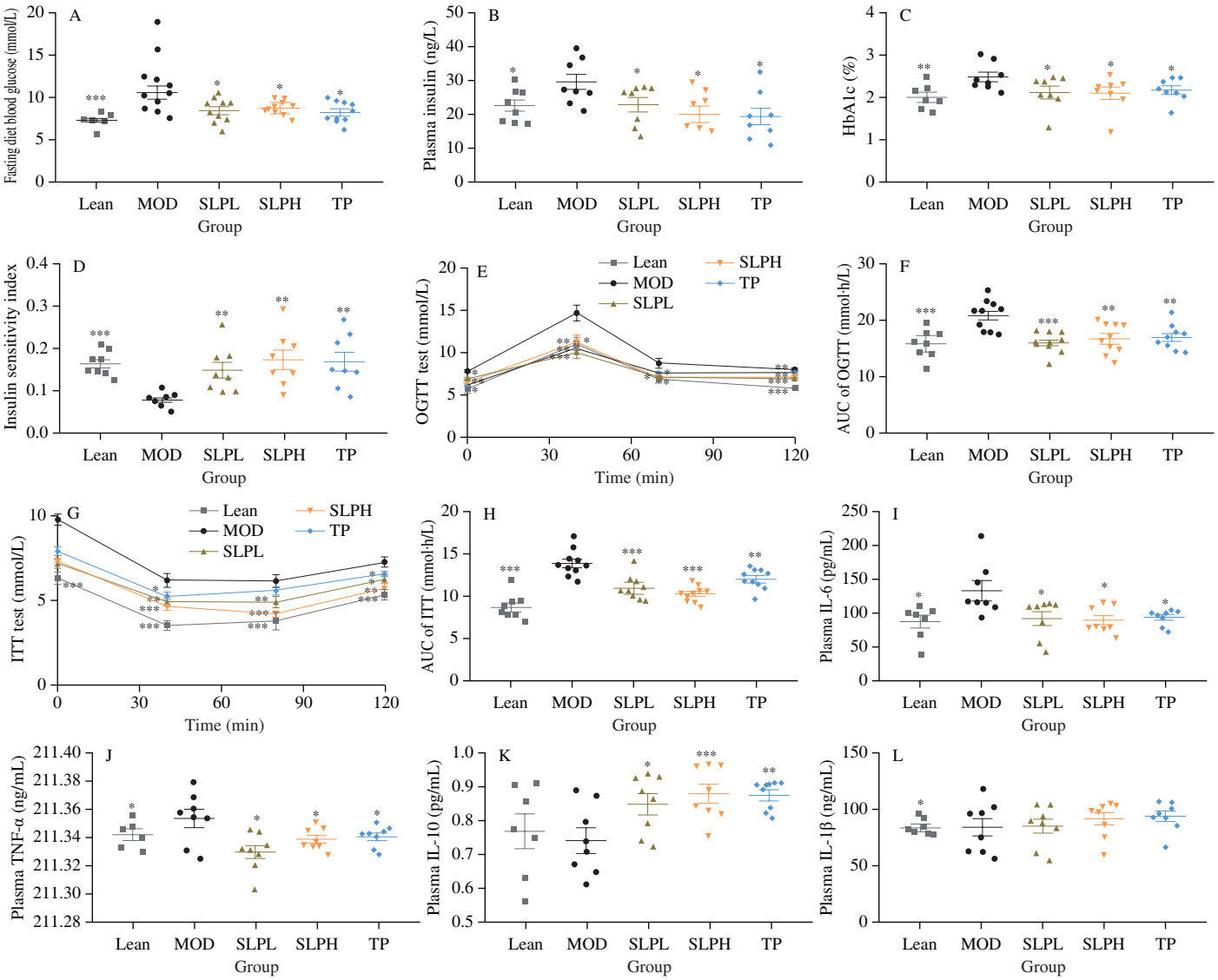

Fig. 3 SLP improved glucose metabolism, decreased inflammation, and metabolic endotoxemia in *ob/ob* mice. *ob/ob* mice were treated with distilled water, TP (50 mg/kg), or SLP (50 mg/kg or 100 mg/kg) for 6 weeks by daily oral gavage. (A) Fasting diet blood glucose; (B) plasma insulin; (C) HbA1c; (D) ISI; (E) OGTT and (F) its mean area under the curve (AUC); (G) plasma glucose profile and (H) mean AUC measured during an ITT; (I) plasma IL-6; (J) plasma TNF-α; (K) plasma IL-10; (L) plasma IL-1β; (M) plasma LPS; (N) relative mRNA level in the ileum ($n = 6$); (O) relative densities of goblet cells; (P) representative AB-PAS staining images in the small intestine. $n = 5$; scale bars, 200 μm and 100 μm. Statistical analysis was analyzed using unpaired Student's *t*-test for (A-D, F, and H-O), and two-way ANOVA followed by the Bonferroni post hoc test for (E and G), $n = 8$–10. $^*P < 0.05$; $^{**}P < 0.01$; $^{***}P < 0.001$.

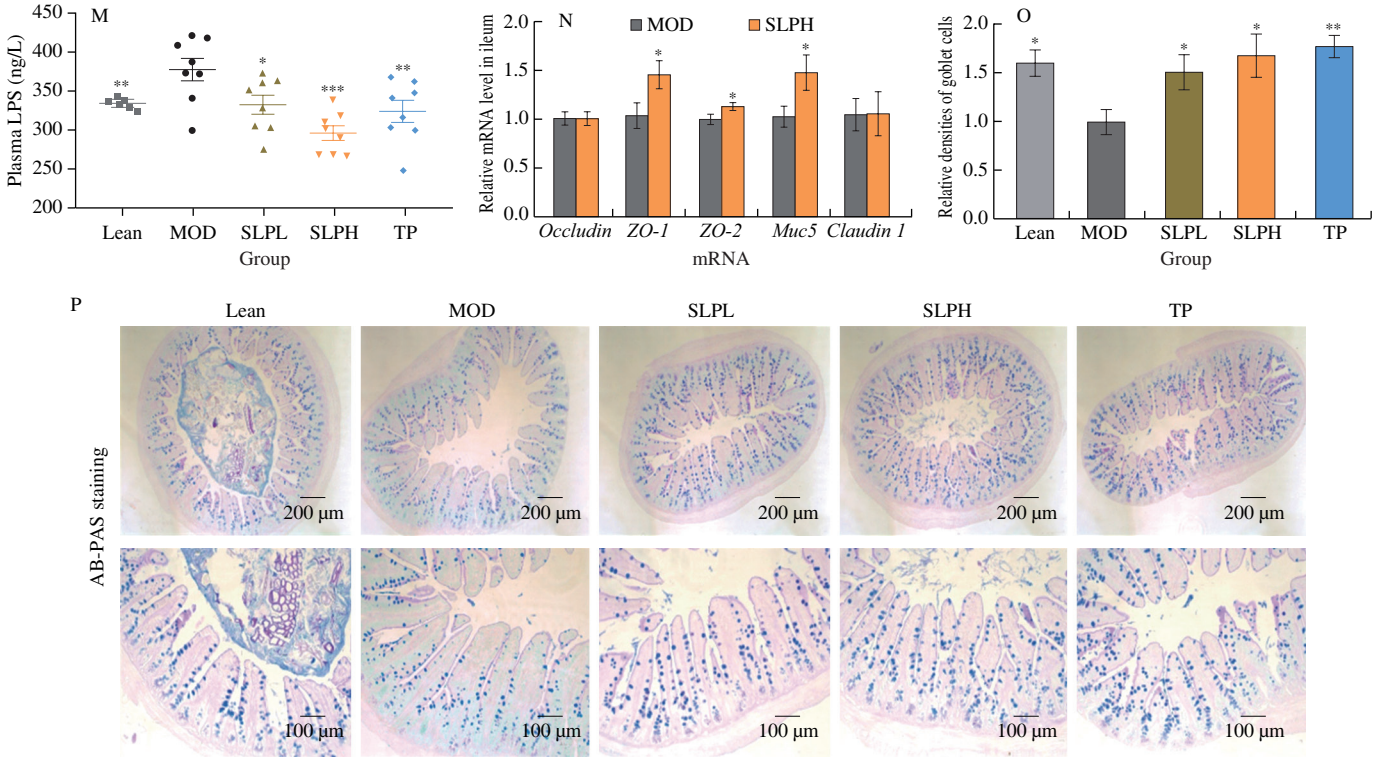

Fig. 3 (*Continued*)

3.4 SLP supplementation modulated gut microbiota composition in ob/ob mice

It has been reported that supplementation with polyphenol-rich diets could ameliorate intestinal dysbiosis and thus confer health-promoting benefits on the host[38]. To assess whether the metabolic protective effects of SLP on *ob/ob* mice were linked with gut microbiota, we compared the composition of gut microbiota in *ob/ob* mice treated with SLP at 100 mg/kg (SLPH) to that of untreated mice (MOD) by performing a 16S rDNA gene-based amplicon sequencing analysis. SLPH and TP supplementation decreased Shannon index and Chao1 index ($P < 0.01$), as compared with the MOD group, indicating SLPH decreased α-diversity (Figs. 4A-B), which is consistent with the report that green tea polyphenol decreased α-diversity[39,40]. Non-metric multidimensional scaling (NMDS) analysis revealed the distinct clustering of gut microbiota composition among the MOD, SLPH, and TP groups (Fig. 4C).

In comparison with the model group, SLPH treatment robustly increased the relative abundance of Bacteroidota ($P = 0.040\ 1$) and Verrucomicrobia ($P < 0.006\ 4$), while decreased the relative abundance of Firmicutes ($P = 0.003\ 6$), Actinobacteria ($P = 0.002\ 2$), Desulfobacterota ($P = 0.015\ 6$) at the phylum levels (Figs. 4D-E). SLPH also reduced the proportion of F/B ratio ($P = 0.014\ 8$) (Fig. 4F). Next, we further studied the alterations of gut microbiota at the genus level upon SLP treatment. In particular, SLPH significantly increased the relative abundances of *Akkermansia* ($P = 0.005\ 5$) and *Bacteroides* ($P = 0.008\ 8$), while largely decreased the relative abundances of the Lachnospiraceae_NK4A136_group ($P = 0.004\ 9$) and *Dubosiella* ($P = 0.046\ 9$) (Figs. 4G-H). At the species level, we observed some obvious changes upon SLPH treatment. Treatment with SLPH greatly enhanced the abundance of *A. muciniphila* ($P = 0.000\ 2$), *B. acidifaciens* ($P = 0.000\ 3$) and *Bacteroides caecimuris* ($P = 0.032\ 4$). TP supplementation significantly increased the abundance of *B. acidifaciens* ($P = 0.041\ 7$), *A. muciniphila* ($P = 0.007\ 6$), *Bacteroides vulgatus* ($P = 0.000\ 5$), and *Bacteroides sarorii* ($P = 0.029\ 5$) (Figs. 4I-J). The above findings demonstrated that SLP could regulate the composition of the gut bacterial community in *ob/ob* mice. Linear discriminant analysis (LDA) effect size (LefSe) analysis was conducted to identify specific gut microbes that accounted for the most remarkable difference under different interventions (Fig. 4K). The results demonstrated that *B. acidifaciens*, *A. muciniphila*, and *B. caecimuris* were enriched in the SLPH-treated group. Similarity percentage procedure (SIMPER) analysis revealed that *B. acidifaciens* (contributors 28.1%) and *A. muciniphila* (contributors 22.8%) were the two largest contributors to the induced alterations by SLPH (Figs. 4L-M). Further, to identify specific gut bacteria that potentially contributed to the anti-MetS efficacy of SLPH, the correlation between the abundance of significantly changed gut bacteria and the key MetS parameters was analyzed by Person's correlation analysis. The commensal bacteria *B. acidifaciens*, *A. muciniphila*, and *B. caecimuris* showed a negative correlation with most MetS phenotypes including plasmatic TG, plasmatic LDL, OGTT, but presented a positive correlation with hepatic T-AOC, SOD, insulin sensitivity index, and plasmatic IL-10 ($P < 0.05$) (Fig. 4N). In conclusion, we speculated that *B. acidifaciens* and *A. muciniphila* were potentially key gut bacteria mediating the beneficial effects of SLP.

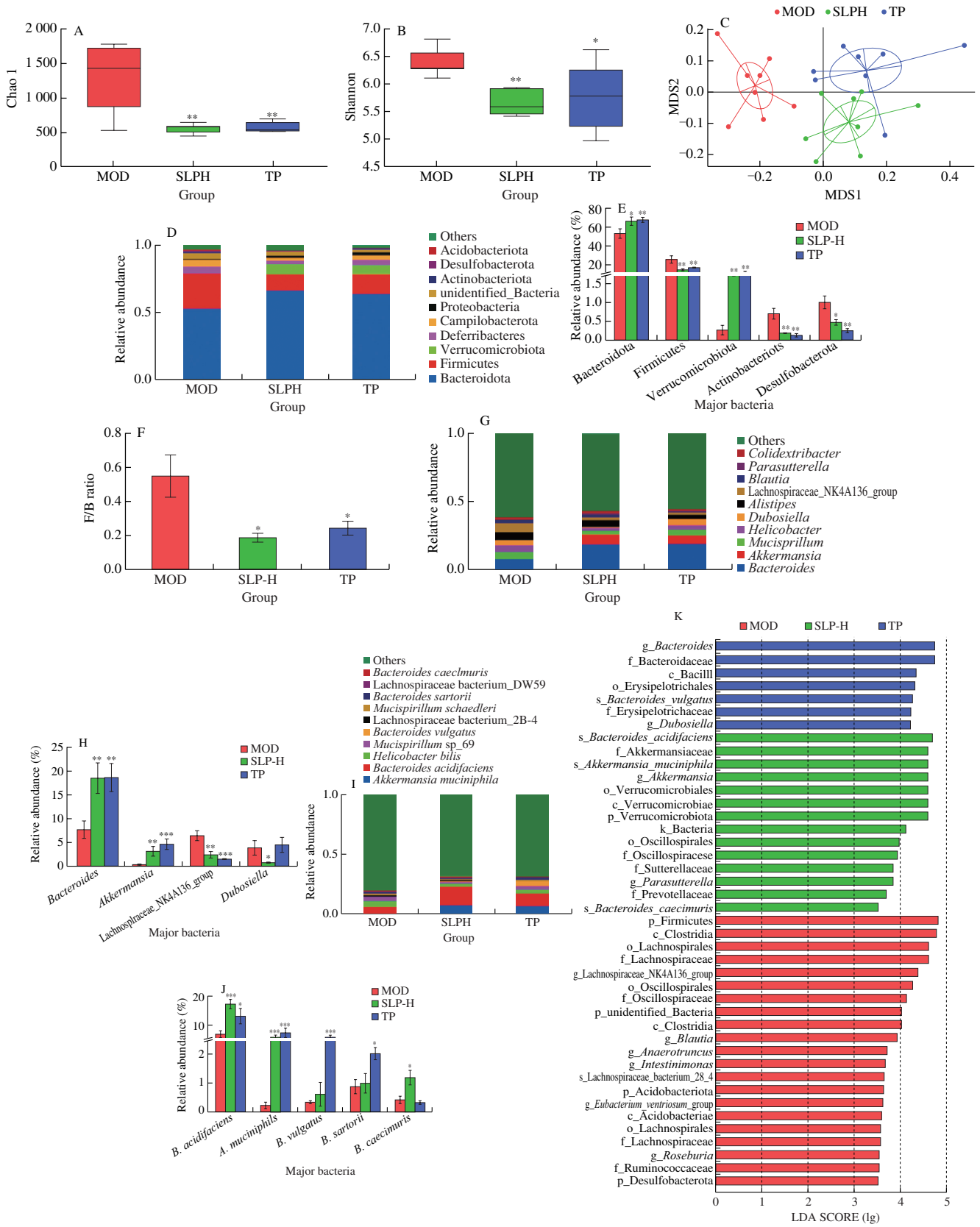

Fig. 4 SLP altered the composition of gut microbiota. *ob*/*ob* mice were treated with distilled water, TP (50 mg/kg), or SLP (100 mg/kg) for 6 weeks by daily oral gavage. (A) Shannon indexes; (B) Chao1 indexes; (C) NMDS; (D-E) the microbial community composition and the relative abundance of major bacteria at phylum level; (F) F/B ratio; (G-H) the microbial community composition and the relative abundance of major bacteria at genus level; (I-J) the microbial community composition and the relative abundance of major bacteria at species level; (K) LefSe analysis. (L, M) the results of SIMPER analysis quantified the contributions of the top 10 different species between the two groups (L, MOD/SLPH; M, MOD/TP), as well as the abundances (percent reads) of these species; (N) Person's correlation analysis between the relative abundance of gut microbiota of the top 10 species and MetS related indices. (E, J and I) were analyzed using one-way ANOVA followed by the Tukey post hoc test, $n = 8$. $^{*}P < 0.05$; $^{**}P < 0.01$; $^{***}P < 0.001$.

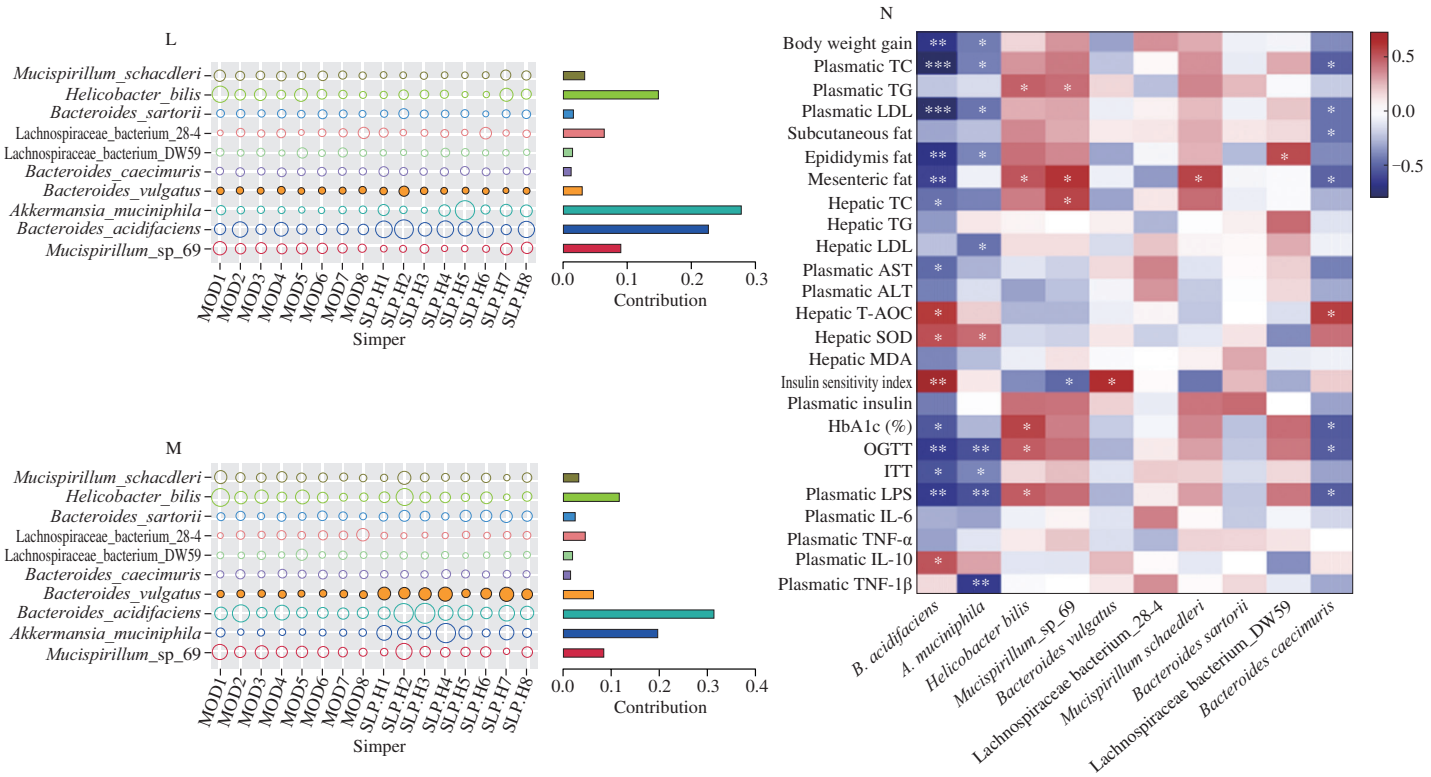

Fig. 4 (*Continued*)

3.5 SLP administration increased the production of gut SCFAs and secondary bile acids, activated brown adipose tissues thermogenesis, and promoted white adipose tissues browning

Polyphenols have been demonstrated to regulate the composition of gut microbiota and reduce metabolic disorders by regulating the microbial-derived metabolites including the production of SCFAs and bile acids[12]. SCFAs was demonstrated to play a vital role in maintaining gut barrier function[41], thus decreasing the level of low-grade inflammation. Compared to the model group (MOD), SCFAs (especially butyrate, propionate, and isopentanoic acid) were increased by oral administration of SLP (Fig. 5A, $P < 0.01$). Among the bile acids, the secondary bile acids, especially β-muricholic acid (β-MCA) ($P = 0.012\ 6$), glycoursodeoxycholic acid (GUDCA) ($P = 0.001\ 4$), 7-ketolithocholic acid (7-keto-LCA) ($P = 0.004\ 5$), 7-oxo-deoxycholic acid (7-keto-DCA) ($P = 0.000\ 5$), and deoxycholic acid (DCA) ($P = 0.003\ 1$) were significantly increased in the feces of SLPH-treated mice in contrast to those of the untreated mice (Fig. 5B).

To understand the mechanisms of SLP on lipid metabolism, we monitored the relative expression of target genes associated with lipogenesis in subcutaneous white adipose tissues (WAT). The expression of acetyl CoA carboxylase-1 (*Acc-1*), fatty acid synthase (*Fas*), and sterol regulatory element-binding protein-1c (*Srebp-1c*) were relatively lower by 13.4%, 16.1%, and 28.5% in the SLPH-treated group (Fig. 5C). We then measured the mRNA expression of thermogenesis-associated genes in WAT and brown adipose tissues (BAT). The results revealed that SLPH administration up-regulated the expression of G protein-coupled receptor 5 (*Tgr5*) ($P = 0.007\ 3$), uncoupling protein 1 (*Ucp1*) ($P = 0.002\ 2$), peroxisome proliferator-activated receptor coactivator-1*a* (*Pgc-1a*) ($P = 0.001\ 1$), and elongation of very-long-chain fatty acids protein 3 (*Elovl-3*) ($P = 0.009\ 5$) in WAT (Fig. 5D). In addition, SLPH markedly increased the expression of *Tgr5* ($P = 0.017\ 6$), *Ucp1* ($P = 0.009\ 5$), *Pgc-1a* ($P = 0.040\ 9$), and the transcription factor PR domain containing 16 (*Prdm16*) ($P = 0.018\ 6$), but did not change the mRNA expression of cell death-inducing DFFA-like effector A (*Cidea*), iodothyronine deiodinase 2 (*Dio2*), and tumor necrosis factor receptor superfamily member 9 (*Cd137*) in BAT (Fig. 5E). It has been addressed that bile acids, like lithocholic acid (LCA), DCA, and chenodeoxycholic acid (CDCA) can improve the activity of BAT and promote the browning of WAT by activating the TGR5 pathway in adipose[42-43]. The above results indicated that the effects of SLP in reducing obesity and hyperlipidemia are mechanisms related to the secondary bile acids-regulated BAT thermogenesis and WAT browning.

3.6 B. acidifaciens and A. muciniphila ameliorated metabolic syndrome in DIO mice

Based on the results of LefSe and SIMPER analysis, *B. acidifaciens* and *A. muciniphila* were chosen for further investigation of the causal relationship between the modulation of gut microbiota and the anti-MetS effects of SLP. To evaluate the efficacy difference between *B. acidifaciens* and *A. muciniphila* and validate the anti-MetS effects of the combination of these two microbes, HFD-induced obese mice were treated with *B. acidifaciens*, *A. muciniphila*, or the combination of the two strains for seven weeks.

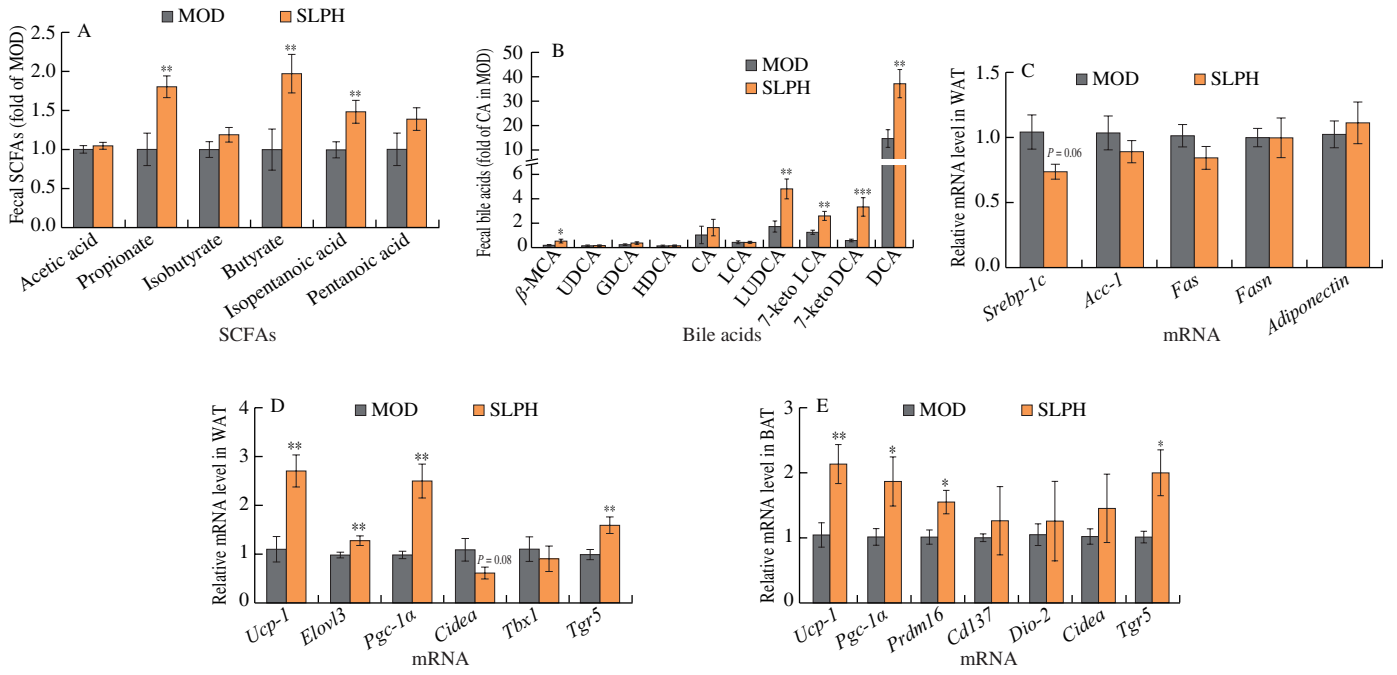

Fig. 5 SLP treatment regulated SCFAs, secondary bile acids metabolism and activated brown adipose tissue thermogenesis, and promoted the browning of white adipose tissues. o*b*/*ob* mice were treated with distilled water or SLP at 100 mg/kg for 6 weeks by daily oral gavage. (A) fecal SCFAs; (B) fecal bile acids (fold of CA in MOD); UDCA, ursodeoxycholic acid; GDCA, glycodeoxycholic acid; HDCA, hyodeoxycholic acid; CA, cholic acid; (C) relative mRNA level in WAT of fatty acid metabolism ($n = 6$); (D) relative mRNA level in WAT ($n = 6$); (E) relative mRNA level in BAT ($n = 6$). Statistical analysis was analyzed using unpaired Student's *t*-test for (A-E), $n = 8$. $^{*}P < 0.05$; $^{**}P < 0.01$; $^{***}P < 0.001$.

In comparison with the HFD-fed mice, the body weight and fat accumulation were greatly decreased in all treated groups ($P < 0.05$), as accompanied by little influence on the food intake (Figs. 6A-D, K). All treatments significantly reduced the concentration of TC and LDL-C in both plasma and liver ($P < 0.05$), while there were little impacts on the levels of plasma and hepatic HDL-C (Figs. 6F-G). Supplementation with *B. acidifaciens* or *A. muciniphila* alone also significantly decreased the levels of TG in the liver and plasma ($P < 0.05$) (Figs. 6E, H). Improvements in liver damages were achieved by all treatments, as indicated by the decreased plasma AST and ALT ($P < 0.05$) as well as oil red O staining of liver sections (Figs. 6I-K). *B. acidifaciens* decreased hepatic LDL-C, hepatic TG, and AST to a greater extent than the other two treatments. In addition, treatment with all the strains largely decreased the levels of free diet blood glucose (*B. acidifaciens*, $P = 0.012\ 0$; *A. muciniphila*, $P = 0.027\ 6$), plasma insulin, HbA1c, inflammatory factors IL-6, TNF-α, and LPS, and intestinal permeability, increased the level of IL-10, ameliorated glucose tolerance and insulin resistance, and enhanced hepatic anti-oxidation ($P < 0.05$) (Figs. 6L-V, X, and S6). The level of IL-1β was less changed in all treated groups (Fig. 6W). Mice treated with *A. muciniphila* or the combination of *B. acidifaciens* and *A. muciniphila* showed more improvement in the gut barrier as well as alleviation of inflammation than the *B. acidifaciens*-treated mice ($P < 0.05$) (Figs. 6Y-AA). In short, we concluded that the colonization with *B. acidifaciens* and *A. muciniphila* effectively ameliorated MetS in DIO mice.

To directly assess the effects of SLP on *B. acidifaciens* and *A. muciniphila*, the growth curves of *B. acidifaciens* and *A. muciniphila* were measured after the addition of SLP in the medium under anaerobic conditions. As a result, the growth of *B. acidifaciens* and *A. muciniphila* was not influenced. Since SLP supplementation greatly elevated the levels of SCFAs and secondary bile acids in the gut of mice, we next detected the SCFAs and secondary bile acids production by *B. acidifaciens* or *A. muciniphila in vitro*. As a result, the concentrations of SCFAs (acetic acid, propionate, butyrate, pentanoic acid, isopentanoic acid, and isobutyrate) were enhanced in the media of *B. acidifaciens* or *A. muciniphila* after 24 h fermentation (Fig. S7), and secondary bile acids including CA, CDCA, 7-keto DCA, and 7-keto LCA were detected in the culture of *B. acidifaciens* with the addition of taurocholic acid (TCA) or taurochenodeoxycholic acid (TCDCA) (Fig. S8). *In vivo* assays indicated that treatment with *A. muciniphila*, *B. acidifaciens*, or the combination of *B. acidifaciens* and *A. muciniphila* increased the levels of propionate, isobutyrate, butyric acid, isopentanoic acid, and pentanoic acid ($P < 0.05$) (Fig. 7A), and supplementation of *B. acidifaciens* or the combination of *B. acidifaciens* and *A. muciniphila* increased the levels of DCA and LCA ($P < 0.05$) (Fig. 7B). Notably, we detected a higher abundance of the fecal GUDA ($P < 0.01$) and 7-keto-DCA ($P < 0.05$) in mice treated with *B. acidifaciens*, *A. muciniphila*, or the combination of two strains. Furthermore, the relative expression of *Ucp1* and *Pgc-1a* were found to be up-regulated ($P < 0.05$) in all bacterial treatments (Fig. 7C). Briefly, we confirm a causal relationship between the gut microbiota modulation and the anti-MetS efficacy of SLP, which is especially correlated with the enrichment of *B. acidifaciens* and *A. muciniphila* as well as their ability in regulating SCFAs and secondary bile acids production in the gut.

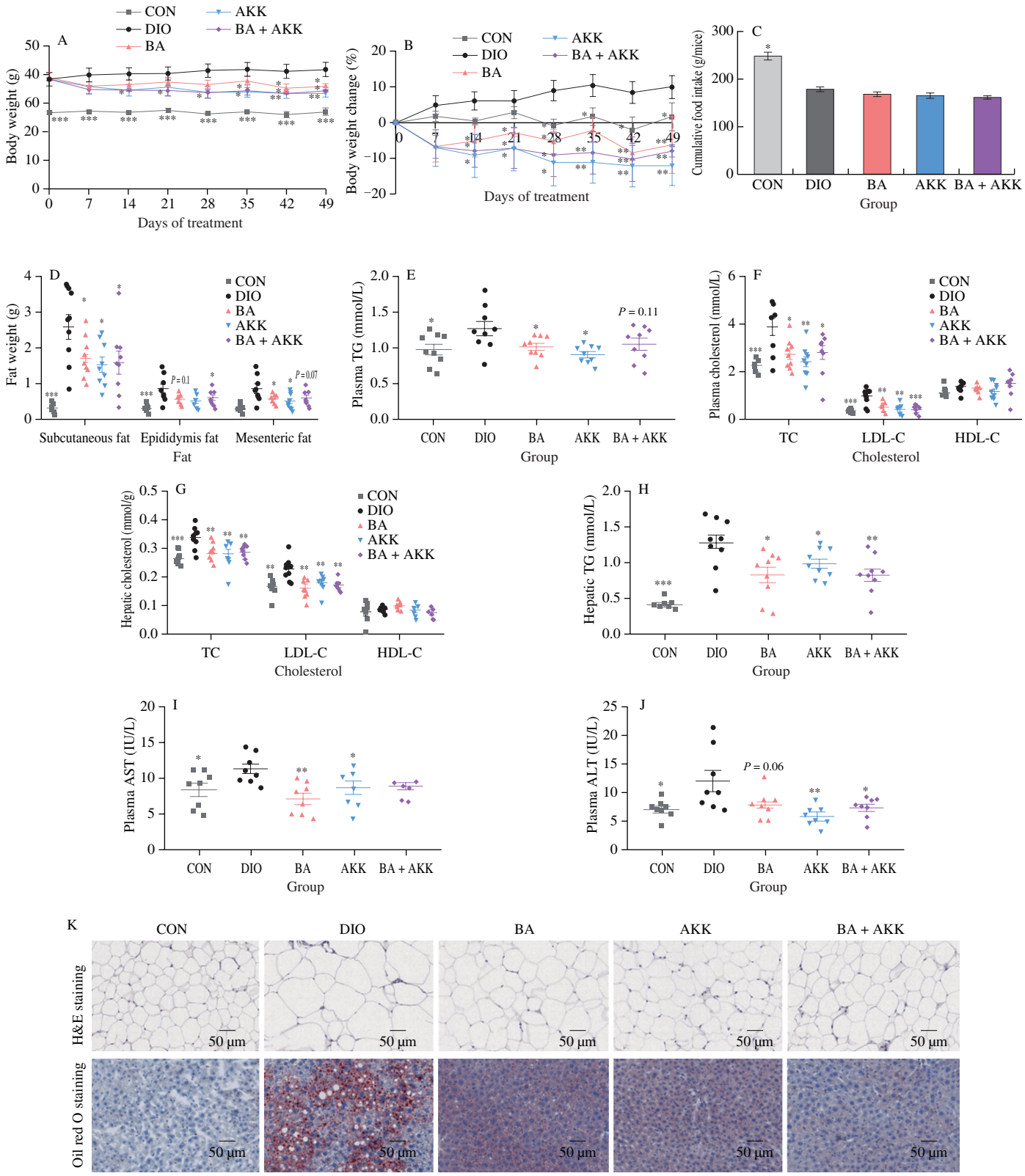

Fig. 6 Administration with *B. acidifaciens*, *A. muciniphila*, or the combination of *B. acidifaciens* and *A. muciniphila* ameliorated metabolic disorders in DIO mice. DIO mice were treated with *B. acidifaciens*, *A. muciniphila,* or a mixture of two bacteria (1×10^8 CFU/mL) for 7 weeks by daily oral gavage. (A) Body weight change during 7 weeks; (B) body weight change; (C) cumulative food intake; (D) fat weight; (E) plasma TG; (F) plasma TC, LDL-C, and HDL-C; (G) hepatic TC, LDL-C, and HDL-C; (H) hepatic TG; (I) plasma AST; (J) plasma ALT; (K) images of H&E staining and oil red O staining in subcutaneous fat and liver, respectively (5 mice per group; scale bars, 50 μm). (L) free diet blood glucose; (M) plasma insulin; (N) ISI; (O) HbA1c; (P) plasma glucose profile and (Q) mean AUC measured during an OGTT; (R) plasma glucose profile and (S) mean AUC measured during an ITT; (T) plasma IL-6; (U) plasma TNF-α; (V) plasma IL-10; (W) plasma IL-1β; (X) plasma LPS; (Y) relative mRNA level in the ileum ($n = 6$); (Z) relative densities of goblet cells ($n = 5$); (AA) images of representative AB-PAS staining in the small intestine. ($n = 5$; scale bars, 200 μm and 100 μm). Statistical analysis was analyzed using unpaired Student's *t*-test for (C-J, L-O, Q, and S-Z), and (A-B, P and R) were using two-way ANOVA followed by the Bonferroni *post hoc* test, $n = 8$–9. $^*P < 0.05$; $^{**}P < 0.01$; $^{***}P < 0.001$.

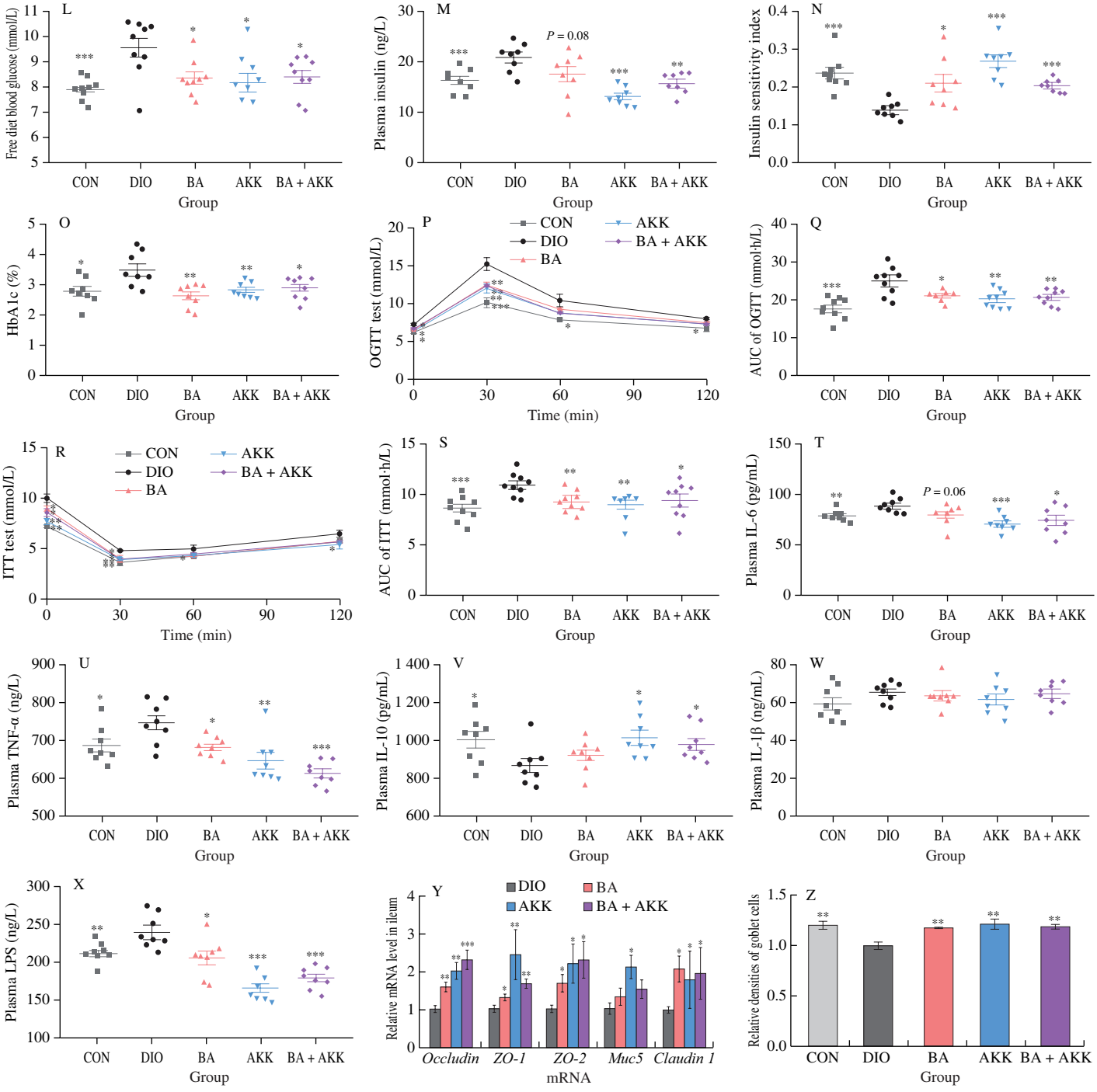

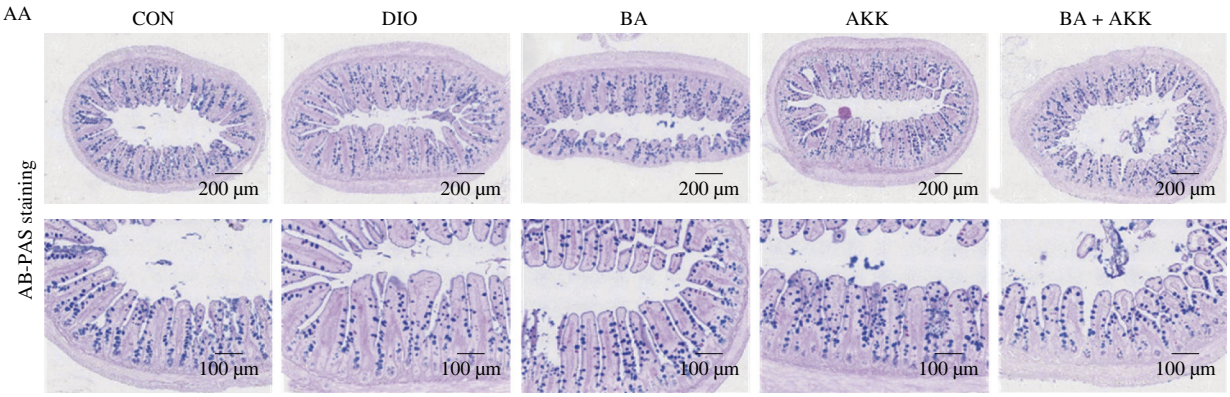

Fig. 6 (*Continued*)

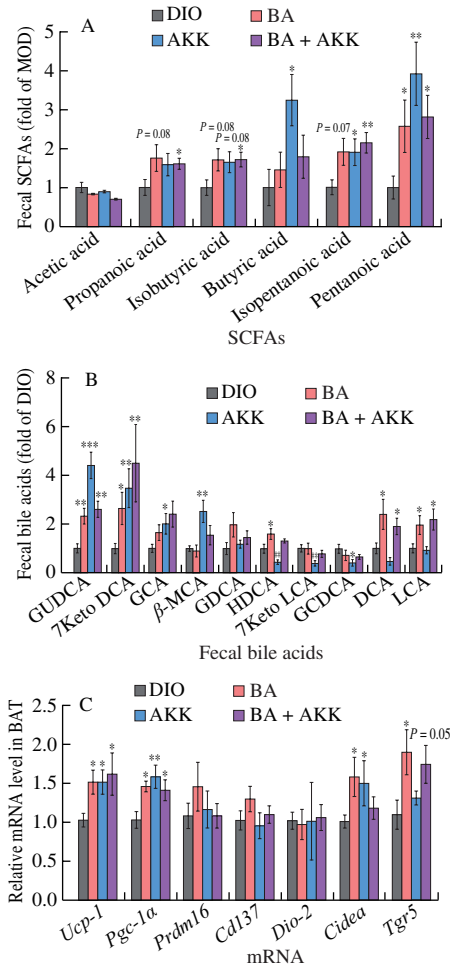

Fig. 7 Administration with *B. acidifaciens*, *A. muciniphila,* or the combination of *B. acidifaciens* and *A. muciniphila* regulated SCFAs and secondary bile acids metabolism in DIO mice. DIO mice were treated with *B. acidifaciens*, *A. muciniphila,* or a mixture of two bacteria (1×10^8 CFU/mL) for 7 weeks by daily oral gavage. (A) fecal SCFAs; (B) fecal bile acids (fold of DIO); GCA, glycocholic acid; GCDCA, glycochenodeoxycholic acid; (C) relative mRNA level in BAT ($n = 6$). (A)-(C) were analyzed using unpaired Student's *t*-test, $n = 9$. $^*P < 0.05$; $^{**}P < 0.01$; $^{***}P < 0.001$.

4. Discussion

Sugarcane leaves have attracted widespread attention due to their health-promoting benefits. Sugarcane leaves are rich in bioactive substances such as polyphenols, polysaccharides, organic acids, lignans, and terpenoids[44] and are used to prepare drinking relieving fever for human beings in some regions of Guangxi Province of China[45-46]. The sugarcane leaves water extracts have been reported to have anti-mutation effect, inhibitory activity on nitric oxide generation, apoptosis-inducing activity on HepG2 cells[47-48], as well as hypoglycemic effect on diabetic mice induced by epinephrine, alloxan, and streptomycin[49]. In this work, we prepared a polyphenol extract from sugarcane leave of Guangxi, China, which was confirmed to contain 4-hydroxybenzaldehyde, *p*-coumaric acid, (*E*)-3-(4-hydroxy-3-methoxyphenyl) acrylic acid, isoviolanthin, (+)-syringaresinol-*O*-*D*-glucopyranoside, tricin-7-*O*-*β*-*D*-glucopyranoside, and tricin-7-*O*-neohesperidoside. Plant-derived phenolic compounds have been widely confirmed as biologically active substances beneficial to body health. Regarding to sugarcane leaves-derived polyphenols, 4-hydroxybenzaldehyde was reported to have anti-inflammatory and anti-platelet aggregation activities[50-51], and *p*-coumaric acid has been shown antioxidant, anti-inflammatory, neuroprotection, and antidiabetic activities[52-55]. A recent study also showed that sugarcane polyphenols and fiber can regulate the composition of gut microbiota and promote the production of SCFAs *in vitro* digestion[56], thus conferring beneficial effects on human health. Herein, we demonstrated that sugarcane leaves-derived polyphenols (SLP) supplementation reduced body weight gain and fat accumulation, ameliorated glucose and lipid metabolisms, and alleviated hepatic steatosis in *ob*/*ob* mice, indicating SLP as good health-promoting substance. This is the first report of the anti-MetS effect for the polyphenol extract of sugarcane leaves. The anti-MetS benefits of SLP was largely correlated with the diverse bioactivities and prebiotic nature of polyphenols.

Chronic low-grade inflammation has been considered as an important pathogenic factor involved in the development of obesity and obesity-associated glucose and lipid metabolism disorders, causing damages to different organs and tissues, such as hepatocyte degeneration, increased fat vacuoles, as well as infiltration in the liver, subcutaneous fat and visceral adipose tissue[57-59]. Our results revealed that SLP treatment significantly decreased the levels of pro-inflammation cytokines (IL-6 and TNF-α) and increased the anti-inflammation cytokines (IL-10), which mechamismly correlated to the reduction of damages in the subcutaneous adipose tissues and liver.

Plant-derived polyphenols, such as tea polyphenols and olive leaf polyphenols, have been demonstrated to reduce MetS by altering the composition of gut microbiota[39,60]. Sugarcane polyphenols were also found to increase SCFA-producing bacteria during *in vitro* digestion and pig fecal fermentation[56]. In this study, we first demonstrated that SLP enriched the commensal bacteria *B. acidifaciens* and *A. muciniphila in vivo*. However, incubation with the addition of SLP did not promote the growth of *B. acidifaciens* and *A. muciniphila in vitro*. Therefore, SLP may stimulate the growth of *B. acidifaciens* and *A. muciniphila* indirectly way. *B. acidifaciens* and *A. muciniphila* shared the same cecum niche because of their similar foraging patterns[61-62]. In early studies, *B. acidifaciens* was demonstrated to enhance insulin sensitivity and improve TGR5/fibroblast growth factor 21 (FGF21)-mediated lipid metabolism[63-64]; *A. muciniphila* was reported to play vital roles in maintaining immune homeostasis and deemed as a promising therapeutic probiotic[9,65].

The gut metabolites were also significantly modulated by SLP in *ob*/*ob* mice. SCFAs, are important metabolites and had recently been confirmed to have therapeutic effects against various metabolic diseases by promoting colonic mucosal health, reducing inflammation, and maintaining glucose homeostasis[41,66]. We validated that *B. acidifaciens* and *A. muciniphila* produce SCFAs *in vitro* and improve intestinal barrier function *in vivo*, thus contributing to the beneficial effects of SLP in intestinal homeostasis. In addition, SLP increased the secondary bile acids, especially *β*-MCA, GUDCA, 7-keto-LCA, 7-keto-DCA, and DCA. Besides, *B. acidifaciens* was demonstrated to convert primary bile acids (TCA or TCDCA) into 7-keto-DCA, and 7-keto LCA, respectively. The BSH and 7*α*-hydroxysteroid dehydrogenases (7*α*-HSDH) activities of *B. acidifaciens* facilitate the biosynthesis of secondary bile acids in the gut of mice. Although unable to transform primary bile acids into

secondary bile acids, *A. muciniphila* can modulate the composition of the gut bacterial community to change the bile acids profile in the gut, which deserves further investigation. Secondary bile acids regulated glucose and lipid metabolism, and energy homeostasis through activating bile acids-specific receptors[67]. LCA and DCA were identified as potent agonists of TGR5. Early studies have demonstrated that the activation of secondary bile acids-TGR5 in BAT was associated with the improvement of MetS[68]. In our study, we observed that SLP administration increased the secondary bile acids levels and activated TGR5 in BAT. The exact mechanisms for the anti-MetS effect of SLP deserve further investigation.

In our experiment, we illustrated that SLP attenuates MetS via regulating the composition of gut microbiota and further increasing the level of SCFAs in the gut, and activating the secondary bile acids-mediated gut-adipose axis. To make full use of sugarcane leaves polyphenols, further studies on humans are demanded.

5. Conclusion

Briefly, the present study showed that polyphenols prepared from sugarcane leaves are rich in flavonoids, phenolic acids, and lignans. Six weeks of SLP supplementation reduced body weight gain and fat accumulation, ameliorated hyperglycemia, hyperlipidemia, and hepatic steatosis, improved gut barrier integrity, and regulated secondary bile acids-mediated BAT thermogenesis and WAT browning in *ob*/*ob* mice. SLP markedly altered the gut microbiota of *ob*/*ob* mice and enriched the gut commensal bacteria *B. acidifaciens* and *A. muciniphila.* Gavage with the above two strains ameliorated MetS in HFD-induced obese mice, confirming the modulation of the gut microbiota as one of the underlying mechanisms for the efficacy of polyphenols from sugarcane leaves. The generation of SCFAs by *B. acidifaciens* and *A. muciniphila* as well as the production of secondary bile acids by *B. acidifaciens* contribute to their metabolic benefits. These results demonstrated that SLP could be a promising functional ingredient to attenuate MetS via regulating gut microbiota.

Declaration of competing interest

Hongwei Liu is an editorial board member for *Food Science and Human Wellness* and was not involved in the editorial review or the decision to publish this article. The authors declare no competing financial interest.

Acknowledgments

This work was supported by the National key research and development program of China (2019YFA0905600), the Science and Technology Service Network Program of the Chinese Academy of Sciences (KFJ-STS-QYZD-201-5-3), and the Strategic Priority Research Program (Class B) of Chinese Academy of Sciences (XDB 38020300).

Appendix A. Supplementary data

Supplementary data associated with this article can be found, in the online version, at http://doi.org/10.26599/FSHW.2022.9250048.

Reference

[1] J. Kaur, A comprehensive review on metabolic syndrome, Cardiol. Res. Pract. 2014 (2014) 943162. https://doi.org/10.1155/2014/943162.
[2] M. Guevara-Cruz, A.G. Flores-Lopez, M. Aguilar-Lopez, et al., Improvement of lipoprotein profile and metabolic endotoxemia by a lifestyle intervention that modifies the gut microbiota in subjects with metabolic syndrome, J. Am. Heart Assoc. 8 (2019) e012401. https://doi.org/10.1161/JAHA.119.012401.
[3] P.J. Miranda, R.A. Defronzo, R.M. Califf, et al., Metabolic syndrome: definition, pathophysiology, and mechanisms, Am. Heart J. 149 (2005) 33-45.
[4] G.M. Saklayen, The global epidemic of the metabolic syndrome, Curr. Hypertens 20 (2018) 12. https://doi.org/10.1016/j.ahj.2004.07.013.
[5] A. Koliada, G. Syzenko, V. Moseiko, et al., Association between body mass index and Firmicutes/Bacteroidetes ratio in an adult Ukrainian population, BMC Microbiol. 17 (2017) 120. https://doi.org/10.1186/s12866-017-1027-1.
[6] P.D. Cani, J. Amar, M.A. Iglesias, et al., Metabolic endotoxemia initiates obesity and insulin resistance, Diabetes 56 (2007) 1761-1772. https://doi.org/10.2337/db06-1491.
[7] J.G. LeBlanc, F. Chain, R. Martin, et al., Beneficial effects on host energy metabolism of short-chain fatty acids and vitamins produced by commensal and probiotic bacteria. Micro, Cell Fact. 16 (2017) 79. https://doi.org/10.1186/s12934-017-0691-z.
[8] S.S. Qiao, K. Wang, C. Liu, et al., The enriched gut commensal *Faecicroseburia intestinalis* contributes to the anti-metabolic disorders effects of the *Ganoderma meroterpene* derivative, Food Sci. Food Saf. 11 (2021) 85-96. https://doi.org/10.1016/j.fshw.2021.07.010.
[9] C. Depommier, A. Everard, C. Druart, et al., Supplementation with *Akkermansia muciniphila* in overweight and obese human volunteers: a proof-of-concept exploratory study, Nat. Med. 25 (2013) 1096. https://doi.org/10.1038/s41591-019-0495-2.
[10] K. Wang, M. Liao, N. Zhou, et al., *Parabacteroides distasonis* alleviates obesity and metabolic dysfunctions via production of succinate and secondary bile acids, Cell Rep. 26 (2019) 222-235. https://doi.org/10.1016/j.celrep.2018.12.028.
[11] H.K. Pedersen, V. Gudmundsdottir, H.B. Nielsen, et al., Human gut microbes impact host serum metabolome and insulin sensitivity, Nature 535 (2016) 376-381. https://doi.org/10.1038/nature18646.
[12] J. Liu, Z. He, N. Ma, et al., Beneficial effects of dietary polyphenols on high-fat diet-induced obesity linking with modulation of gut microbiota, J. Agri. Food Chem. 68 (2019) 33-47. https://doi.org/10.1021/acs.jafc.9b06817.
[13] F. Huang, X. Zheng, X. Ma, et al., Theabrownin from pu-erh tea attenuates hypercholesterolemia via modulation of gut microbiota and bile acid metabolism, Nat. Commun. 10 (2019) 4971. https://doi.org/10.1038/s41467-019-12896-x.
[14] P. Wang, J. Gao, W. Ke, et al., Resveratrol reduces obesity in high-fat diet-fed mice via modulating the structure and metabolic function of the gut microbiota, Free Radic. Biol. Med. 156 (2020) 83-98. https://doi.org/10.1016/j.freeradbiomed.2020.04.013.
[15] G. Matacchione, F. Gurau, S. Baldoni, et al., Pleiotropic effects of polyphenols on glucose and lipid metabolism: focus on clinical trials, Ageing Res. Rev. 61 (2020) 101074. https://doi.org/10.1016/j.arr.2020.101074.
[16] R.V. Santos, A.R. Evangelista, J.C. Pinto, et al., Chemical composition of sugar cane (*Saccharum* spp.) and of the silages with different additives at two cutting ages, Cienc. Agrotecnologia 30 (2006) 1184-1189. https://doi.org/10.1590/S1413-70542006000600022.
[17] Y.T. Xu, C.Y. Li, X.B. Huang, et al., Photoinduced hydroxylation of arylboronic acids with molecular oxygen under photocatalyst-free conditions, Green Chem. 21 (2019) 4971-4975. https://doi.org/10.1039/C9GC02229E.
[18] S. Moussouni, C.V. Karakousi, P. Tsatalas, et al., Biological studies with phytochemical analysis of cornus mas unripe fruits, Chem. Nat. Compd. 56 (2020) 141-144. https://doi.org/10.1007/s10600-020-02966-8.
[19] R. Swisłocka, M. Kowczyk-Sadowy, M. Kalinowska, et al., Spectroscopic (FT-IR, FT-Raman, ^{1}H and ^{13}C NMR) and theoretical studies of *p*-coumaric acid and alkali metalp-coumarates, Spectroscopy 27 (2012) 35-48. https://doi.org/10.3390/molecules20023146.
[20] J.M. Gieel, I. Serbian, A. Loesche, et al., Substituted cinnamic anhydrides act as selective inhibitors of acetylcholinesterase, Bioorg. Chem. 90 (2019) 103058. https://doi.org/10.1016/j.bioorg.2019.103058.
[21] J. Shuai, Z. Li, S. Wei, et al., Bioactive constituents of *Glycyrrhiza uralensis* (Licorice): discovery of the effective components of a traditional herbal medicine, J. Nat. Prod. 79 (2017) 281-292. https://doi.org/10.1021/acs.jnatprod.5b00877.
[22] T. Deyama, T. Ikawa, S. Nishibe, et al., The constituents of *Eucommia ulmoides* OLIV. II. Isolation and structures of three new lignan glycosides, Chem. Pharm. Bull. 33 (1985) 3651-3657. https://doi.org/10.1248/cpb.33.3651.
[23] W.X. Sun, X. Li, N. Li, et al., Chemical constituents of the extraction of bamboo leaves from *Phyllostachys nigra* (Lodd. ex Lindl.) Munro var. *henonis* (Mitf.) Stepf. ex Rendle, J. Shenyang Pharm. Univ. 25 (2008) 39-43. https://doi.org/10.1631/jzus.B0820047.
[24] J. Zhang, Y. Wang, X.Q. Zhang, et al., Chemical constituents from the leaves of *Lophatherum gracile*, Chin. J. Nat. Med. 7 (2010) 428-431. https://doi.org/10.3724/SP.J.1009.2009.00428.

[25] J. Yang, K.X. Liu, J.M. Qu, et al., The changes induced by cyclophosphamide in intestinal barrier and microflora in mice, Eur. J. Pharmacol. 714 (2013) 120-124. https://doi.org/10.1016/j.ejphar.2013.06.006.
[26] L. Sun, L. Bao, D. Phurbu, et al., Amelioration of metabolic disorders by a mushroom-derived polyphenols correlates with the reduction of Ruminococcaceae in gut of DIO mice, Food Sci. Hum. Well. 10 (2021) 442-451. https://doi.org/10.1016/j.fshw.2021.04.006.
[27] Q. Christian, P. Elmar, Y. Pelin, et al., The SILVA ribosomal RNA gene database project: improved data processing and web-based tools, Nucleic Acids Res. 41 (2012) D590-D596. https://doi.org/10.1093/nar/gks1219.
[28] R.C. Edgar, MUSCLE: multiple sequence alignment with high accuracy and high throughput, Nucleic Acids Res. 32 (2004) 1792-1797. https://doi.org/10.2460/ajvr.69.1.82.
[29] Q. Wang, G.M. Garrity, J.M. Tiedje, et al., Naive bayesian classifier for rapid assignment of rRNA sequences into the new bacterial taxonomy, Appl. Environ. Microbiol. 73 (2007) 5261-5267. https://doi.org/10.1128/AEM.00062-07.
[30] W. Shi, H. Qi, Q. Sun, et al., gcMeta: a global catalogue of metagenomics platform to support the archiving, standardization and analysis of microbiome data, Nucleic Acids Res. 47 (2019) D637-D648. https://doi.org/10.1093/nar/gky1008.
[31] C. Lapierre, A. Voxeur, S. Boutet, et al., Arabinose conjugates diagnostic of ferulate-ferulate and ferulate-monolignol cross-coupling are released by mild acidolysis of grass cell walls, J. Agri. Food Chem. 67 (2019) 12962-12971. https://doi.org/10.1021/acs.jafc.9b05840.
[32] H.E. Robert, M.G. Scott, Z.Z. Paul, Metabolic syndrome, Lancet 365 (2005) 1415-1428. https://doi.org/10.1016/S0140-6736(05)66378-7.
[33] B. Msa, C. Fa, D. Gma et al., Role of polyphenols in combating type 2 diabetes and insulin resistance, Int. J. Biol. Macromol. 206 (2022) 567-579. https://doi.org/10.1016/j.ijbiomac.2022.03.004.
[34] C.S. Yang, J.S. Zhang, L. Zhang, et al., Mechanisms of body weight reduction and metabolic syndrome alleviation by tea, Mol. Nutr. Food Res. 60 (2016) 160-174. https://doi.org/10.1002/mnfr.201500428.
[35] C.S. Yang, J. Hong, Prevention of chronic diseases by tea: possible mechanisms and human relevance, Annu. Rev. Nutr. 33 (2013) 161-181. https://doi.org/10.1146/annurev-nutr-071811-150717.
[36] A. Kashani, A.D. Brejnrod, C. Jin, et al., Impaired glucose metabolism and altered gut microbiome despite calorie restriction of *ob*/*ob* mice, Animal Microbiome 1 (2019) 1-16. https://doi.org/10.1186/s42523-019-0007-1.
[37] C.P. Briscoe, D. Looper, P. Tran, et al., LPS-induced biomarkers in mice: a potential model for identifying insulin sensitizers, Biochem. Bioph. Res. Co. 361 (2007) 140-145. https://doi.org/10.1016/j.bbrc.2007.06.164.
[38] J.R. Marchesi, D.H. Adams, F. Fava, et al., The gut microbiota and host health, Gut 65 (2015) 330-339. https://doi.org/10.1136/gutjnl-2015-309990.
[39] J. Zhou, L.L. Tang, C.L. Shen, et al., Green tea polyphenols modify gut-microbiota dependent metabolisms of energy, bile constituents and micronutrients in female sprague-dawley rats, J. Nutr. Biochem. 61 (2018) 68-81. https://doi.org/10.1016/j.jnutbio.2018.07.018.
[40] T. Chen, A.B. Liu, S. Sun, et al., Green tea polyphenols modify the gut microbiome in *db*/*db* mice as co-abundance groups correlating with the blood glucose lowering effect, Mol. Nutr. Food Res. 63 (2019) 1801064. https://doi.org/10.1002/mnfr.201801064.
[41] J. Tan, C. McKenzie, M. Potamitis, et al., The role of short-chain fatty acids in health and disease, Adv. Immunol. 121 (2014) 91-119. https://doi.org/10.1016/B978-0-12-800100-4.00003-9.
[42] E.P. Broeders, E.B. Nascimento, B. Havekes, et al., The bile acid chenodeoxycholic acid increases human brown adipose tissue activity, Cell Metab. 22 (2015) 418-426. https://doi.org/10.1016/j.cmet.2015.07.002.
[43] A. Molinaro, A. Wahlstrom, H.U. Marschall, Role of bile acids in metabolic control, Trends Endocrinol Metab. 29 (2018) 31-41. https://doi.org/10.1016/j.tem.2017.11.002.
[44] R. Colombo, F.M. Lancas, J.H. Yariwake, et al., Determination of flavonoids in cultivated sugarcane leaves, bagasse, juice and in transgenic sugarcane by liquid chromatography-UV detection, J. Chromatogr. A 1103 (2006) 118-124. https://doi.org/10.1016/j.chroma.2005.11.007.
[45] C. Sun, Summer-heat relieving flour suitable for eating in summer and preparation method thereof, (2013) CN103349038A.
[46] S.X. Xu, The invention relates to sugarcane leaves tea beverage and a preparation method thereof, (2012) CN102823677B.
[47] C.P. Lee, Z.T. Chen, P.Y. Yu, et al., Identification of bioactive compounds and comparison of apoptosis induction of three varieties of sugarcane leaves, J. Funct. Foods 4 (2012) 391-397. https://doi.org/10.1016/j.jff.2012.01.011.
[48] B.S. Wang, P.D. Duh, S.C. Wu, et al., Effects of the aqueous extract of sugarcane leaves on antimutation and nitric oxide generation, Food Chem. 124 (2010) 495-500. https://doi.org/10.1016/j.foodchem.2010.06.060.
[49] X.T. Hou, J.G. Deng, A.Y. Li, et al., Study on hypoglycemia activity of the different extracts of sugarcane leaves, West China J. Pharm. Sci. 26 (2011) 451-453. https://doi.org/10.13375/j.cnki.wcjps.2011.05.011.
[50] X.F. Li, R. Dai, G.H. Li, et al., Anti-platelet aggregation function and acute toxicity of 4-hydroxybenzyl aldehyde(4-HBAL) extracted from *Gastrodia elata* Blume, Nat. Prod. Res. Dev. 25 (2013) 317-320. https://doi.org/10.16333/j.1001-6880.2013.03.006.
[51] B. Xiang, S. Liu, Y. Guo, et al., Study of anti-inflammation of *p*-hydroxybenzaldehyde from *Gastrodia elata* Blume, Chin. J. Ethnomed. Ethnopharm. 25 (2016) 16-19. https://doi.org/CNKI:SUN:MZMJ.0.2016-09-010.
[52] A. Abdel-Moneim, A.I. Yousef, S.A. El-Twab, et al., Gallic acid and *p*-coumaric acid attenuate type 2 diabetes-induced neurodegeneration in rats, Metabolic Brain Disease 32 (2017) 1279-1286. https://doi.org/10.1007/s11011-017-0039-8.
[53] J.H. Yoon, K. Youn, C.T. Ho, et al., *p*-Coumaric acid and ursolic acid from *Corni Fructus* attenuated β-amyloid25–35-induced toxicity through regulation of the NF-κB signaling pathway in PC12 cells, J. Agri. Food Chem. 62 (2014) 4911-6. https://doi.org/10.1021/jf501314g. Epub 2014 May 19.
[54] M. Guven, A.B. Aras, T. Akman, et al., Neuroprotective effect of *p*-coumaric acid in rat model of embolic cerebral ischemia, Iran. J. Basic Med. Sci. 18 (2015) 356-363.
[55] S.A. Yoon, K. Seong, S. Hye-Sun, et al., *p*-Coumaric acid modulates glucose and lipid metabolism via AMP-activated protein kinase in L6 skeletal muscle cells, Biochem. Bioph. Res. Co. 432 (2013) 553-557. https://doi.org/10.1016/j.bbrc.2013.02.067.
[56] Y.T. Loo, K. Howell, H. Suleria, et al., Sugarcane polyphenol and fiber to affect production of short-chain fatty acids and microbiota composition using *in vitro* digestion and pig faecal fermentation model, Food Chem. 385 (2022) 132665. https://doi.org/10.1016/j.foodchem.2022.132665.
[57] P. Paresh, A. Aljada, A. Chaudhuri, et al., Metabolic syndrome: a comprehensive perspective based on interactions between obesity, diabetes, and inflammation, Circulation 111 (2005) 1448-1454. https://doi.org/10.1161/01.CIR.0000158483.13093.9D.
[58] R. Cancello, K. Clément, Is obesity an inflammatory illness? Role of low-grade inflammation and macrophage infiltration in human white adipose tissue, BJOG 113 (2006) 1141-1147. https://doi.org/10.1111/j.1471-0528.2006.01004.x.
[59] S.P. Weisberg, D. McCann, M. Desai, et al., Obesity is associated with macrophage accumulation in adipose tissue, J. Clin. Invest. 112 (2003) 1796-1808. https://doi.org/ 10.1172/JCI19246.
[60] B. Tva, C. Rn, A. Fa, et al., The metabolic and vascular protective effects of olive (*Olea europaea* L.) leaf extract in diet-induced obesity in mice are related to the amelioration of gut microbiota dysbiosis and to its immunomodulatory properties, Pharmacol. Res. 150 (2019) 104487. https://doi.org/10.1016/j.phrs.2019.104487.
[61] D. Berry, B. Stecher, A. Schintlmeister, et al., Host-compound foraging by intestinal microbiota revealed by single-cell stable isotope probing, P. Natl. Acad. Sci. U.S.A. 110 (2013) 4720-4725. https://doi.org/10.1073/pnas.1219247110.
[62] D. Berry, E. Mader, T.K. Lee, et al., Tracking heavy water (D_2O) incorporation for identifying and sorting active microbial cells, P. Natl. Acad. Sci. U.S.A. 112 (2014) 194-203. https://doi.org/10.1073/pnas.1420406112.
[63] J.Y. Yang, Y.S. Lee, Y. Kim, et al., Gut commensal *Bacteroides acidifaciens* prevents obesity and improves insulin sensitivity in mice, Mucosal Immunol. 10 (2016) 104-116. https://doi.org/10.1038/mi.2016.42.
[64] L. Wu, Q. Yan, F. Chen, et al., Bupleuri radix extract ameliorates impaired lipid metabolism in high-fat diet-induced obese mice via gut microbia-mediated regulation of FGF21 signaling pathway, Biomed. Pharmacother. 135 (2021) 111187. https://doi.org/10.1016/j.biopha.2020.111187.
[65] A. Everard, C. Belzer, L. Geurts, et al., Cross-talk between *Akkermansia muciniphila* and intestinal epithelium controls diet-induced obesity, P. Natl. Acad. Sci. U.S.A. 110 (2013) 9066-9071. https://doi.org/10.1073/pnas.1219451110.
[66] S.S, Qiao, K. Wang, C. Liu, et al., The enriched gut commensal *Faeciroseburia intestinalis* contributes to the anti-metabolic disorders effects of the *Ganoderma* meroterpene derivative, Food Sci. Hum. Well. 11 (2022) 85-96. https://doi.org/10.1016/j.fshw.2021.07.010.
[67] T. Pols, L.G. Noriega, M. Nomura, et al., The bile acid membrane receptor TGR5: a valuable metabolic target, Digest. Dis. 29 (2011) 37-44. https://doi.org/10.1159/000324126.
[68] L.A. Velazquez-Villegas, A. Perino, V. Lemos, et al., TGR5 signalling promotes mitochondrial fission and beige remodelling of white adipose tissue, Nat. Commun. 9 (2018) 245. https://doi.org/10.1038/s41467-017-02068-0.